On canonical triangulations of once-punctured torus bundles and two-bridge link complements

FRANÇOIS GUÉRITAUD
APPENDIX A BY DAVID FUTER

We prove the hyperbolization theorem for punctured torus bundles and two-bridge link complements by decomposing them into ideal tetrahedra which are then given hyperbolic structures, following Rivin's volume maximization principle.

57M50; 57M27

À la mémoire de Pierre Philipps

1 Introduction

Let $T := (\mathbb{R}^2 \smallsetminus \mathbb{Z}^2)/\mathbb{Z}^2$ be the once-punctured torus endowed with its differential structure and an orientation. The group G of isotopy classes of orientation-preserving diffeomorphisms $\varphi\colon T \to T$ (or the mapping class group of T) is identified as $G \simeq \mathrm{SL}_2(\mathbb{Z})$, so each such map φ has well-defined eigenvalues in $\mathbb{C}$. For $[\varphi]$ in G, define the *punctured torus bundle*

$$V_\varphi := T \times [0,1]/\sim$$

where $\sim$ identifies $(x,0)$ with $(\varphi(x),1)$ for all x in T. Then V_φ is a differentiable oriented 3–manifold, well-defined up to diffeomorphism. Thurston's Hyperbolization Theorem [21] implies the following theorem as a very special case.

Theorem 1.1 *If φ has two distinct real eigenvalues, the punctured torus bundle V_φ admits a finite-volume, complete hyperbolic metric.*

The aim of this paper is to prove Theorem 1.1 by elementary and, to some extent, constructive arguments. The strategy is to exhibit a canonical, geodesic triangulation $\mathcal{H}$ of V_φ into ideal tetrahedra (hyperbolic tetrahedra whose vertices are at infinity).

Combinatorially, $\mathcal{H}$ (sometimes called the Floyd–Hatcher or monodromy triangulation) is found by expressing a certain conjugate of $\pm\varphi$ as a product of positive transvection matrices. Once such combinatorial data for a triangulation is given, the problem of

Published: 16 September 2006 DOI: 10.2140/gt.2006.10.1239

making it hyperbolic lends itself to two approaches. One is complex, explicit and "local": cross-ratio computations, particular hyperbolic isometries, etc (see eg Neumann and Zagier [20]). The other approach, first described by Rivin [22], de Verdière [25] and Casson, is real-analytic and "global": in order to make the structure complete, one kills its monodromy by maximizing the total hyperbolic volume (but combinatorial obstructions might arise). In the case of V_φ, the combinatorial structure of $\mathcal{H}$ is sufficiently well-understood to allow a nice interplay between the two approaches, yielding useful "medium-range" results (Section 8). The philosophy of such results is that if the structure with maximal volume is noncomplete, it should still be complete at "most" places, enabling us to make geometric statements.

Akiyoshi [4], combining the methods of Akiyoshi, Sakuma, Wada and Yamashita [5] and Minsky [18], proved that the "combinatorially canonical" triangulation $\mathcal{H}$ must also be "geometrically canonical," ie topologically dual to the Ford–Voronoi domain of V_φ. Lackenby [13], assuming the existence of the hyperbolic metric, derived the same result by a normal surface argument. In [10], we apply the methods of the present paper to extend the Akiyoshi–Lackenby theorem to quasifuchsian groups (where pleating laminations of the convex core replace the attractive and repulsive laminations of the monodromy φ).

Knowing the space of angle structures also allows for easy volume estimates, some of which are worked out in the Appendix: these estimates make the constants of Brock [8] explicit (and sharp) for the class of manifolds under consideration. Although the main results of the present paper are known, our ambition is to demonstrate that hyperbolic geometry and combinatorics (of the curve complex, say) can interact more intimately than at the level of coarse geometry, a phenomenon which seems to extend beyond punctured torus groups and begs to be further explored. Other references closely related to this subject include the beautiful article of Akiyoshi, Sakuma, Wada and Yamashita [6], which builds on the work of Jørgensen and partly motivated our work [10], and the examples compiled in Alestalo and Helling [7], Helling [11] and Koch [12].

The converse of Theorem 1.1 is true. If the trace τ of the monodromy map φ is in $\{-1, 0, 1\}$, then $[\varphi]$ has finite order and V_φ is Seifert fibered. If $\tau = \pm 2$, then φ preserves a nontrivial simple closed curve γ (parallel to a rational eigenvector) in the punctured torus, and γ defines an incompressible torus or Klein bottle in V_φ. In any case we get a topological obstruction to the existence of the hyperbolic metric.

An attempt to be self-contained will be made in proving Theorem 1.1. The proof will deal primarily with the case where the eigenvalues of φ are positive. The other case is only a minor variant (in particular, $V_{-\varphi}$ can be obtained by ungluing the metric tetrahedra of V_φ and regluing them in a slightly different way).

Section 2 is standard and recalls the classification of conjugacy classes in $\mathrm{SL}_2(\mathbb{Z})$ in order to define the triangulation $\mathcal{H}$. The latter is studied in greater detail in Section 3 and Section 4. Positive angles for $\mathcal{H}$ (a "linear hyperbolic structure") are provided in Section 5. Section 6 explains the role played by hyperbolic volume maximization, allowing us to deal with the easy cases in Section 7. Section 8 presents the essential geometric lemma for the final attack, carried out in Section 9. Section 10 is devoted to a numerical example. In Section 11, we quickly recall the connection between once-punctured tori and 4–punctured spheres. In the Appendix, David Futer builds on that connection to prove an analogue of Theorem 1.1 for the complements of two-bridge links and computes geometric estimates.

The symbol "=" is preceded (resp. followed) by a colon (:=, resp. =:) when the equality serves as a definition for its left (resp. right) member.

I would like to thank Francis Bonahon and Frédéric Paulin for numerous insights and the great improvements this paper owes to them. Exciting discussions with David Futer and with Makoto Sakuma also gave invaluable input. This paper reached its pre-final form during a stay at the Institut Bernoulli (EPFL, Lausanne) for whose kind hospitality I express my deep gratitude. Finally, thanks are due to the referee for many helpful comments. This work was partially supported by NSF grant DMS-0103511.

2 Conjugacy in $\mathrm{SL}_2(\mathbb{Z})$ and the Farey tesselation

Proposition 2.1 *Let φ be an element of $\mathrm{SL}_2(\mathbb{Z})$ with two distinct eigenvalues in $\mathbb{R}_+^*$. Then the conjugacy class of φ in $\mathrm{SL}_2(\mathbb{Z})$ contains an element of the form*

$$A\varphi A^{-1} = \begin{pmatrix}1 & a_1\\ 0 & 1\end{pmatrix}\begin{pmatrix}1 & 0\\ b_1 & 1\end{pmatrix}\begin{pmatrix}1 & a_2\\ 0 & 1\end{pmatrix}\begin{pmatrix}1 & 0\\ b_2 & 1\end{pmatrix}\cdots\begin{pmatrix}1 & a_n\\ 0 & 1\end{pmatrix}\begin{pmatrix}1 & 0\\ b_n & 1\end{pmatrix}$$

where $n>0$ and the a_i and b_i are positive integers. Moreover, the right hand side is unique up to cyclic permutation of the factors $\left(\begin{smallmatrix}1 & a_i\\ 0 & 1\end{smallmatrix}\right)\left(\begin{smallmatrix}1 & 0\\ b_i & 1\end{smallmatrix}\right)$. Conversely, any nonempty product of such factors is an element of $\mathrm{SL}_2(\mathbb{Z})$ with two distinct eigenvalues in $\mathbb{R}_+^*$.

We sketch a proof of this popular fact, mainly in order to introduce the *cyclic word* Ω associated to φ. The converse implication is easy (just check that the trace is larger than 2), so we focus on the direct statement.

Consider the upper half-plane model of the hyperbolic plane $\mathbb{H}^2$, endowed with the Farey tessellation F (the ideal triangle 01∞ iteratedly reflected in its sides). We identify $\mathrm{PSL}_2(\mathbb{R})$ with the group of isometries of $\mathbb{H}^2$ *via* the isomorphism Ψ defined

by

$$\Psi\begin{pmatrix} a & b \\ c & d \end{pmatrix} : z \mapsto \frac{dz+c}{bz+a}.$$

(Under this slightly unusual convention, the slopes of the eigenvectors of M are the fixed points of $\Psi(M)$, rather than their inverses as would normally be the case.) It is known that the group of orientation-preserving isometries of $\mathbb{H}^2$ preserving F is thus identified with $\mathrm{PSL}_2(\mathbb{Z})$.

If D is the oriented hyperbolic line running from the repulsive fixed point of $\pm\varphi$ to the attractive one, then D crosses infinitely many Farey triangles $(\dots t_{-1}, t_0, t_1, t_2, \dots)$ of F. We can formally write down a bi-infinite word

$$\Omega = \dots LRRRLLR \dots$$

where the k–th letter is R (resp. L) if D exits t_k to the Right (resp. Left) of where it enters. We will also say that D *makes a Right* (resp. *Left*) at t_k. The word Ω contains at least one R and one L, because the ends of D are distinct. The image of t_0 under φ is a certain t_m $(m > 1)$, and Ω is periodic of period m.

Next, define the standard transvection matrices

$$R := \begin{pmatrix} 1 & 1 \\ 0 & 1 \end{pmatrix} \quad \text{and} \quad L := \begin{pmatrix} 1 & 0 \\ 1 & 1 \end{pmatrix}.$$

These are parabolic transformations of $\mathbb{H}^2$ whose respective fixed points are 0 and ∞. Let M be any subword of Ω of length m: we see M as a product of standard transvection matrices, and therefore as an element of $\mathrm{SL}_2(\mathbb{Z})$. By studying the actions of R and L on F, it is then easy to see that φ and M are conjugates in $\mathrm{PSL}_2(\mathbb{Z})$, and therefore in $\mathrm{SL}_2(\mathbb{Z})$ since both have positive trace. This proves the existence statement for the (a_i, b_i).

Uniqueness is checked as follows: on one hand, if φ and φ' are conjugates, a certain element of $\mathrm{PSL}_2(\mathbb{Z})$ (preserving F) takes the axis of φ to the axis of φ', so they define the same word Ω up to translation. On the other hand, looking at the actions of R and L on $\mathbb{H}^2$, one sees that a product of standard transvection matrices (as in the statement of Proposition 2.1) will define the word $\Omega = R^{a_1}L^{b_1}\dots R^{a_n}L^{b_n}$, concatenated infinitely many times with itself.

In the language of Proposition 2.1, the sequence $(a_1, b_1, \dots, a_n, b_n)$ can be shown to be (a positive power of) the period of the continued fraction expansion of the slope of the expanding eigenvector of φ. The word Ω will be seen either as infinite periodic, or as finite cyclic, depending on the context.

3 The canonical triangulation

3.1 Diagonal exchanges

There is another well-known interpretation of the Farey tessellation F of the hyperbolic plane $\mathbb{H}^2$. Under the canonical identification $H_1(T,\mathbb{Z}) \simeq \mathbb{Z}^2$, where T is the punctured torus defined in the Introduction, each rational number in the boundary $\widehat{\mathbb{R}} = \mathbb{R} \cup \{\infty\}$ of $\mathbb{H}^2$ can be seen as a *slope*, ie a proper isotopy class of properly embedded lines in T, going from the puncture to itself. The action of $\mathrm{SL}_2(\mathbb{Z})$ on $\widehat{\mathbb{Q}}$ coincides with the action of the mapping class group G of T on rational slopes. The edges of the Farey tessellation F connect exactly the pairs of rational numbers whose corresponding slopes, or curves in T, can be homotoped off each other (away from the puncture). The faces of F, having three edges, correspond exactly to the isotopy classes of *ideal triangulations* of T: any such triangulation has one vertex (the puncture), three edges, and two triangles (which meet along each edge). As one crosses from a face of F to one of its neighbors, exactly one vertex gets replaced, which in the corresponding triangulations of T means that exactly one edge is changed. Inspection shows that the triangulation must be undergoing a *diagonal exchange*: erase one edge e, thus liberating a quadrilateral space Q of which e was a diagonal, then insert back the other diagonal.

3.2 Tetrahedra

As before, let φ be an element of $\mathrm{SL}_2(\mathbb{Z})$ with two distinct eigenvalues in $\mathbb{R}_+^*$. In the proof of Proposition 2.1, we introduced the triangles $t_0, t_1, \dots$ crossed by the axis D of φ. In view of the above, this yields a nonbacktracking path of diagonal exchanges between some triangulation (associated to t_0) and its pushforward by φ (associated to t_m).

More precisely, when the oriented line D crosses an edge e of the Farey tessellation, e comes with a transverse orientation. So we can define the *top* (resp. *bottom*) triangulation $\tau_+(e)$ (resp. $\tau_-(e)$) of the punctured torus T as being the one associated with the Farey triangle crossed just after (resp. before) the edge e. A diagonal exchange separates the triangulations $\tau_-(e)$ and $\tau_+(e)$. An ideal tetrahedron is by definition a space diffeomorphic to an ideal hyperbolic tetrahedron (topologically it is a compact tetrahedron with its vertices removed). We can immerse such an ideal tetrahedron $\Delta(e)$ in $T \times \mathbb{R}$: the boundary of the immersed $\Delta(e)$ is made up of two *pleated surfaces* (top and bottom) homotopic to T and triangulated according to $\tau_+(e)$ and $\tau_-(e)$ respectively (Figure 1). The immersion is an embedding on the interior of $\Delta(e)$, but two pairs of opposite edges undergo identifications.

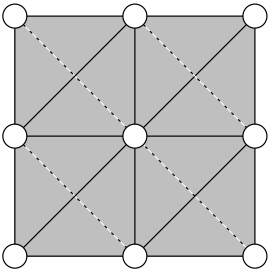

Figure 1: Four copies of $\Delta(e)$ in the cover $(\mathbb{R}^2 \smallsetminus \mathbb{Z}^2) \times \mathbb{R}$ of $T \times \mathbb{R}$

Next, if D crosses the Farey edges $e_i, e_{i+1}, \dots$, we can glue the top of the tetrahedron $\Delta_i := \Delta(e_i)$ onto the bottom of Δ_{i+1} in $T \times \mathbb{R}$, because $\tau_+(e_i) = \tau_-(e_{i+1})$. We thus get a bi-infinite stack of tetrahedra $(\Delta_i)_{i \in \mathbb{Z}}$. For any nonnegative N the space $U_N := \bigcup_{i=-N}^{N} \Delta_i$ is a strong deformation retraction of $T \times \mathbb{R}$. For N large enough, U_N is homeomorphic to $T \times [0,1]$: the only way this can fail is if all the Δ_i for $-N \le i \le N$ have a common edge; but any edge of any tetrahedron Δ_j is shared by only finitely many other (consecutive) Δ_i's, because for any Farey vertex v, only finitely many of the Farey edges e_i bound triangles with v as a vertex (and these e_i are consecutive). Therefore, the space $U = \bigcup_{i \in \mathbb{Z}} \Delta_i$ is homeomorphic to $T \times \mathbb{R}$. If m is the period of the word Ω, there is an orientation-preserving homeomorphism Φ of U, acting like $[\varphi]$ on the T–factor, that sends Δ_i to Δ_{i+m} for all i. The quotient U/Φ is a manifold (homeomorphic to) V_φ, naturally triangulated into m ideal tetrahedra.

Figure 2 also shows a way to interpret the standard transvection matrices R and L directly as adjunctions of new tetrahedra (by performing diagonal exchanges on the top faces). Similarly, to topologically triangulate a general pseudo-Anosov surface bundle, we can always go by diagonal exchanges from some triangulation (of the surface) to its pushforward by the monodromy map, an idea usually credited to Casson.

4 Combinatorics of the torus at infinity

The manifold V_φ is naturally homeomorphic to the interior of a compact manifold with boundary, denoted by $\overline{V}_\varphi$ and defined as a bundle over the circle with fiber $T - \delta$, where δ is a regular neighborhood of the puncture.

The *torus at infinity* of the manifold V_φ is the boundary of $\overline{V}_\varphi$, namely a topological torus. The links of the vertices of the tetrahedra Δ_i provide a tessellation $\mathcal{A}$ of the torus at infinity into topological triangles. In this section we investigate the combinatorics of $\mathcal{A}$.

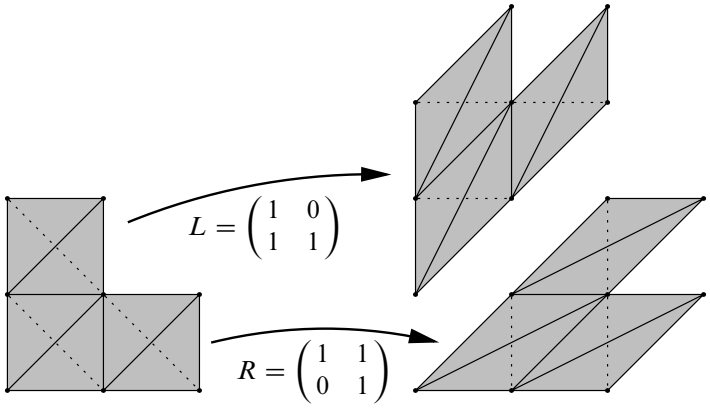

Figure 2

Each vertex of $\mathcal{A}$ corresponds to an edge of V_φ shared by a few consecutive tetrahedra Δ_i. This edge in turn corresponds to a Farey vertex shared by a few consecutive Farey triangles. The union of all the Farey triangles adjacent to a given vertex v forms a *fan*. If v arises as a vertex of triangles visited by the oriented line D, one of the following two things must happen right after D enters the fan: either D makes a Right, then a number of Lefts (possibly 0), then a Right and leaves the fan; or the same is true, exchanging Right and Left.

Therefore, the vertices of $\mathcal{A}$ correspond exactly to the subwords of Ω of the form RL^*R or LR^*L (where $* \geq 0$). Each such subword actually corresponds to two vertices of $\mathcal{A}$, because the edges of the tetrahedra Δ_i have two ends.

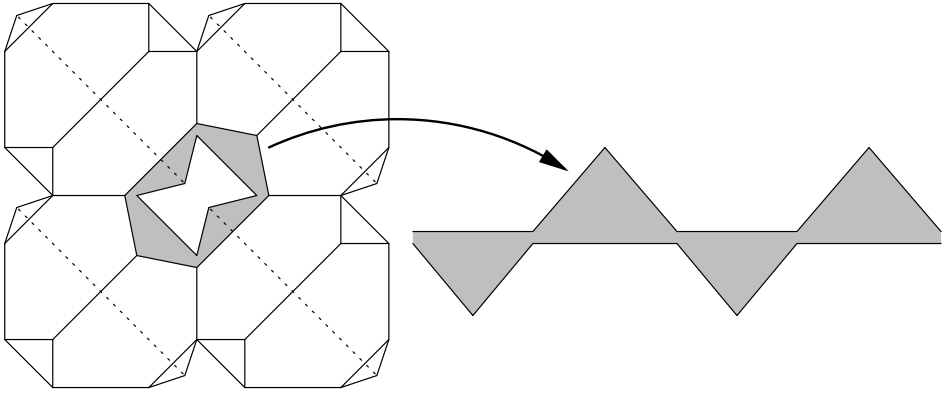

Figure 3: The link of the puncture

Moreover, each tetrahedron Δ_i, having four vertices, contributes exactly four triangles to $\mathcal{A}$. By looking at a vertex (puncture) of the cover $(\mathbb{R}^2 \smallsetminus \mathbb{Z}^2) \times \mathbb{R}$ of $T \times \mathbb{R}$ with embedded Δ_i, one checks (Figure 3) that each of the four triangles has exactly one vertex not shared with any of the other three: we call this vertex the *apex* and the opposite edge the *base*. The four bases form a broken line of four segments which is a closed curve running around the puncture, and the four apices point alternatively up and down in the $\mathbb{R}$–factor. Such chains of four triangles must be stacked on top of one another while respecting the previously described combinatorics of the vertices. The result is shown in Figure 4, where the underlying word Ω was chosen to be $\dots R^4 L^4 R^4 L^4 \dots$ (read from bottom to top). A few remarks are in order.

First remark We labeled by x_i, y_i, z_i the angular sectors of the triangles corresponding to the tetrahedron Δ_i (in Figure 4, the subscript i is replaced by a number at the center of the triangle, omitted after the first few levels). Each angular sector corresponds to a (topological) dihedral angle of Δ_i. Opposite dihedral angles are equal in ideal hyperbolic tetrahedra: this is why three different labels per level are enough (instead of six, the total number of edges in a tetrahedron).

Second remark The design in Figure 4 of the vertices of the torus at infinity, represented as being "opened up", is intended to emphasize the layered structure of the picture (each layer corresponds to one tetrahedron Δ_i).

Third remark Proving Theorem 1.1 by the method outlined in the Introduction amounts to realizing Figure 4 geometrically in the plane by Euclidean triangles, making same-layer angles with identical labels equal (Lemma 6.2 will make this statement more precise).

Fourth remark The convention is that the pair of edges of Δ_i that does not get identified into one edge is labeled z_i: so z_i is the label at the apex (in the sense of Figure 3). Equivalently, if a tetrahedron is seen as a diagonal exchange, z_i is the label common to the appearing and disappearing edges. The other edge pairs are labeled in such a way that in each triangle the letters x, y, z appear *clockwise* in that order. Therefore, if e_i is a Farey edge and p (resp. q) its right (resp. left) end for the transverse orientation, the dihedral angle of the tetrahedron Δ_i at the edge of slope p (resp. q) is x_i (resp. y_i).

Fifth remark The tetrahedra Δ_i are naturally indexed in $\mathbb{Z}/m\mathbb{Z}$. The letters R and L live naturally on the pleated surfaces, or *between* the tetrahedra Δ_i. In Figure 4 and henceforth, the i–th layer is colored in grey if and only if the letters just before and

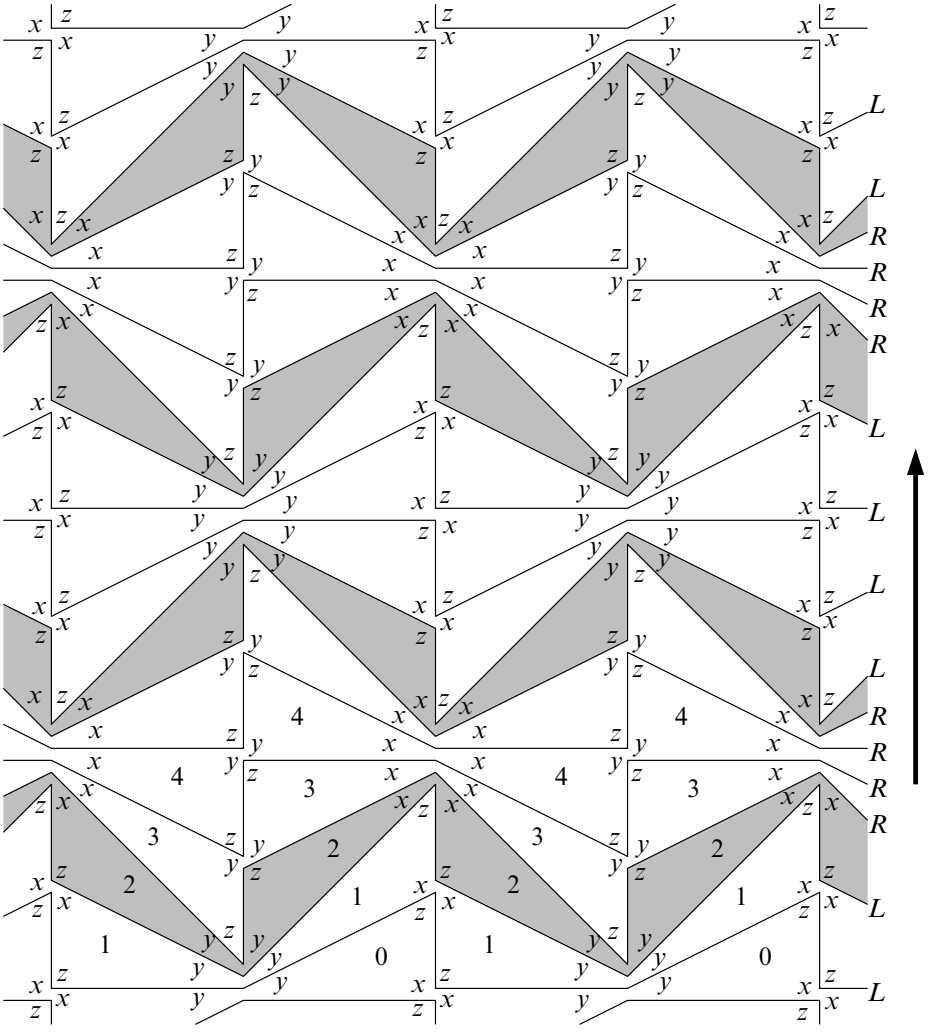

Figure 4: The tessellation $\mathcal{A}$

just after Δ_i are different (here $i = 2, 6, \dots$). Such indices i are called *hinge* indices, because they are at the hinge between two nonempty subwords R^p and L^q. Hinge tetrahedra (the associated Δ_i) will play an important role later on.

Sixth remark While the fundamental domain of Figure 4 is supposed to have a horizontal length of four triangles (see Figure 3), we notice a horizontal period of length only two. This corresponds to the "hyperelliptic" involution of the once-punctured

fiber torus (rotation of 180° around the puncture, central in $\mathrm{SL}_2(\mathbb{Z})$ and therefore well-defined on V_φ). This will simplify many of our computations.

Seventh remark The valence of a vertex s corresponding to a subword RL^nR or LR^nL of Ω (where $n \geq 0$) is $2n+4$. This is because exactly $n+2$ Farey triangles are adjacent to the corresponding rational v_s; each such Farey triangle defines a triangulated surface (with an edge of slope v_s), and each such surface contributes exactly two segments issuing from s in $\mathcal{A}$.

5 Finding positive angles

The tetrahedra Δ_i and Δ_{i+1} have two common triangular faces whose union forms a *pleated punctured torus* Σ properly isotopic to $T \times \{*\}$ in $T \times \mathbb{R}$. Moreover, Σ receives a transverse "upward" orientation from the $\mathbb{R}$–factor. Suppose all tetrahedra Δ_i are endowed with dihedral angles. Let e be an edge of Σ: if the sum of all dihedral angles at e *below* Σ is $\pi + \alpha$, we call α the *pleating angle* of Σ at e.

In this section we find positive dihedral angles for the ideal tetrahedra Δ_i. More precisely, we describe the convex space Π of positive angles x_i, y_i, z_i for the Δ_i such that:

(1)
$$\begin{cases} \text{i} — \text{For each } i \text{ in } \mathbb{Z}/m\mathbb{Z} \text{ one has } x_i + y_i + z_i = \pi; \\ \text{ii} — \text{The dihedral angles around any edge add up to } 2\pi; \\ \text{iii} — \text{For each } i \text{ in } \mathbb{Z}/m\mathbb{Z}, \text{ the three pleating angles of the pleated} \\ \qquad \text{punctured torus between } \Delta_i \text{ and } \Delta_{i+1} \text{ add up to } 0. \end{cases}$$

Condition (1)-ii is necessary, though not sufficient, for a hyperbolic structure at the edges; Condition (1)-iii is necessary, though not sufficient, to make the loop around the puncture of T a parabolic isometry of $\mathbb{H}^3$ (see Sublemma 6.4). This "cusp condition" (1)-iii restricts the space of angle structures, but will make it a little easier to describe.

Recall the line D that runs from the repulsive fixed point q^- to the attractive fixed point q^+ of φ across the Farey triangulation. If the tetrahedron Δ_i, corresponding to the Farey edge e_i, realizes a diagonal exchange that erases an edge ε' and replaces it with ε, we denote by z_i the interior dihedral angle of Δ_i at ε and ε' by the fourth remark following Figure 4. Observe that the slope of ε (resp. ε') is the rational located opposite e_i in the Farey diagram, on the side of q^+ (resp. q^-). We define the *half pleating angle* w_i by $\pi - 2w_i = z_i$.

Thus, if (1)-ii and (1)-iii are to be satisfied, the pleating angles of the pleated punctured torus Σ living between Δ_i and Δ_{i+1} must be

(2)
$$-2w_i, \quad 2w_{i+1} \quad \text{and} \quad 2w_i - 2w_{i+1}.$$

(Observe the signs: by our definition, angles pointing upwards, like the "new" edge of Δ_i, are negative pleatings, while angles pointing downwards, like the "old" edge of Δ_{i+1}, are positive ones.) We write the numbers (2) in the corners of the corresponding Farey triangle (top of Figure 5), distinguishing the cases L and R, and we repeat this for all indices i.

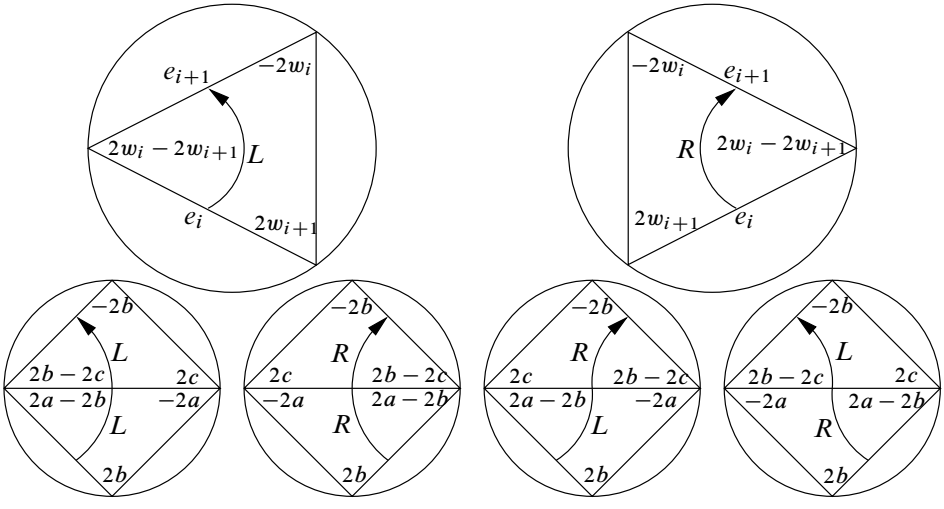

Figure 5: On the bottom row in each case, e_i is the horizontal edge

In fact, the values of the w_i will also determine the x_i and y_i. To see this, we must write down the pleating angles of *two* pleated surfaces, living above *and* below the tetrahedron Δ_i. For notational convenience, write

$$(w_{i-1}, w_i, w_{i+1}) =: (a, b, c).$$

By the fourth remark following Figure 4, the quantity $2x_i$ (resp. $2y_i$) is the difference between the numbers written just above and just below the right (resp. left) end of e_i in Figure 5 (the factor 2 comes from the fact that the two edges of Δ_i with angle x_i (resp. y_i) are identified). By computing differences between the pleating angles given in Figure 5 (bottom), we find the formulae in Table 1 for x_i, y_i, z_i (depending on the letters Ω_i^- and Ω_i^+, each equal to R or L, living respectively just before and just after the index i).

Ω_i^-, Ω_i^+	$L\ L$	$R\ R$	$L\ R$	$R\ L$
x_i	$a+c$	$-a+2b-c$	$a+b-c$	$-a+b+c$
y_i	$-a+2b-c$	$a+c$	$-a+b+c$	$a+b-c$
z_i	$\pi-2b$	$\pi-2b$	$\pi-2b$	$\pi-2b$

Table 1

Condition (1)-i can be checked immediately, while (1)-ii-iii are true by construction. From Table 1, the conditions for all angles x_i, y_i, z_i to be positive are that:

$$(3)\quad \begin{cases} \text{i} — \text{For all } i \text{ one has } 0 < w_i < \pi/2. \\ \text{ii} — \text{If } i \text{ is not a hinge index (first two cases), } 2w_i > w_{i+1} + w_{i-1}. \\ \text{iii} — \text{If } i \text{ is a hinge index (last two cases), } |w_{i+1} - w_{i-1}| < w_i. \end{cases}$$

We call (3)-i the *range* condition, (3)-ii the *concavity* condition, and (3)-iii the *hinge* condition. The space P of sequences $(w_i)_{i\in\mathbb{Z}/m\mathbb{Z}}$ which satisfy (3), homeomorphic to the solution space Π of (1), is clearly an open, convex polyhedron of compact closure in $\mathbb{R}^m$. Moreover, P is nonempty: to exhibit a sequence (w_i) in P, set $w_j = \pi/3$ when j is a hinge index, and complete the gaps between consecutive hinge indices $j < k$ with strictly concave subsequences taking their values in $[\pi/3, \pi/2)$, eg $w_i = \pi/3 + \frac{(i-j)(k-i)}{(k-j)^2}$ for $j \le i \le k$ (indices are of course seen in $\mathbb{Z}$ for the evaluation). Figure 6 shows the typical graph of a sequence (w_i) that satisfies all conditions of (3). Finally, note that the formulae of Table 1 are still valid when Ω is reduced to RL or LR (the letters a and c are just two names for the same parameter then).

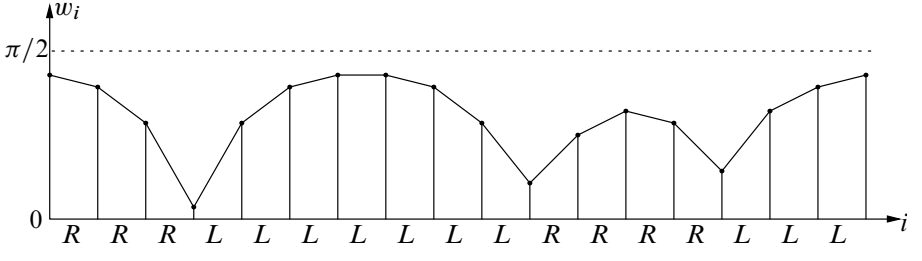

Figure 6

6 Hyperbolic volume

Our goal for the remainder of the paper is to find a point (w_i) of P where the tetrahedra fit together so as to yield a complete hyperbolic structure on V_φ. This section is devoted to checking that this is the same as finding in P a critical point of the total hyperbolic volume, an approach pioneered by Rivin [22]. A few facts concerning the volume of ideal tetrahedra will be needed.

6.1 Volume of an ideal tetrahedron

The volume of a hyperbolic tetrahedron whose dihedral angles are $x, y, z > 0$ is

$$\mathcal{V}(x,y,z) = -\int_0^x \log(2\sin u)\,du - \int_0^y \log(2\sin u)\,du - \int_0^z \log(2\sin u)\,du \tag{4}$$

(we refer to Milnor [17] for a proof). Since $\int_0^\pi \log(2\sin u)\,du = 0$, Equation (4) easily implies the following proposition.

Proposition 6.1 *The function $\mathcal{V}$ can be continuously extended by 0 to all nonnegative triples (x,y,z) such that $x+y+z=\pi$. If $\frac{d}{dt}(x_t,y_t,z_t) = (X,Y,Z)$ then*

$$\exp\left(\frac{-d}{dt}\mathcal{V}(x_t,y_t,z_t)\right) = \sin^X x_t \sin^Y y_t \sin^Z z_t. \tag{5}$$

Proof Straightforward. We will always apply this formula exactly in the form it is stated, because it will usually make the right hand side simplest. □

6.2 Critical volume and trivial holonomy

Lemma 6.2 (Rivin, Chan–Hodgson) *On the open affine polyhedron P of sequences (w_i) satisfying (3), define the volume functional $\mathcal{V}$ as the sum of the hyperbolic volumes of tetrahedra Δ_i with dihedral angles x_i, y_i, z_i, as given by Table 1. Then (w_i) is a critical point for $\mathcal{V}$ in P if and only if the gluing of the tetrahedra Δ_i defines a complete finite-volume hyperbolic structure on the punctured torus bundle V_φ.*

Proof This now standard fact holds for general ideal triangulations as well (see for example Chan [9] or Rivin [22]). The following proof, however, is deliberately specific to the example at hand. This will enable us to introduce a few objects and relationships that will be useful in the sequel. Conversely, the main idea of the present proof (associate to each edge of V_φ an explicit deformation in the space of angle structures) can be used to prove the general case of Rivin's theorem.

First we assume (w_i) is critical. Let B be the torus at infinity of V_φ with the vertices of the tessellation $\mathcal{A}$ removed. Let σ be the hyperelliptic involution of the fiber T, so σ acts as a translation on B. Define $B' = B/\sigma$ and $\mathcal{A}' = \mathcal{A}/\sigma$. Let t_0 be a triangle of $\mathcal{A}'$, ϵ_0 an oriented edge of t_0 and x_0 an interior point of t_0. The group of orientation-preserving similarities of the Euclidean plane $\mathbb{C}$ is $\mathbb{C}^* \ltimes \mathbb{C}$.

Definition 6.3 For a given (w_i) in P, the *holonomy function* is the representation

$$\rho\colon \pi_1(B', x_0) \to \mathbb{C}^* \ltimes \mathbb{C}$$

defined as follows. Given an element α of $\pi_1(B', x_0)$, view α as a cyclic sequence of triangles $t_0, t_1, \dots, t_s = t_0$ of $\mathcal{A}'$, such that any two consecutive t_i's share an edge. Then, draw an oriented copy τ_0 of t_0 in the plane $\mathbb{C}$, with angles specified by (w_i), by making the image of the oriented edge ϵ_0 coincide with $(0, 1)$. Sharing an edge with τ_0, draw a copy τ_1 of t_1, also with angles specified by (w_i). Then draw a copy τ_2 of t_2 adjacent to τ_1, etc. By definition, $\rho(\alpha)$ is the orientation-preserving similarity mapping the copy of the oriented edge ϵ_0 in τ_0 to the copy of ϵ_0 in τ_s. The *reduced holonomy function* $\psi\colon \pi_1(B', x_0) \to \mathbb{C}^*$ is defined as the projection of ρ on the first factor.

It is a simple exercise to check that ρ is well-defined, and is a representation (the concatenation rule being that $\alpha\beta$ denotes the path α followed by the path β). Note that ψ, having a commutative target, factors through a representation $\psi\colon H_1(B', \mathbb{Z}) \to \mathbb{C}^*$.

Sublemma 6.4 *Let α be an element of $H_1(B', \mathbb{Z})$ represented by a curve around a 4–valent vertex of $\mathcal{A}'$, and let β be represented by a curve that follows a "grey" (hinge) level in $\mathcal{A}'$ (Figure 7). If (w_i) is critical for the volume functional $\mathcal{V}$, then $\psi(\alpha) = \psi(\beta) = 1$.*

Proof We already know that $\psi(\alpha), \psi(\beta)$ belong to $\mathbb{R}_+^*$, since the angle conditions (1) defining P impose oriented parallelism. It remains to prove that $|\psi(\alpha)| = |\psi(\beta)| = 1$.

At a critical point, the partial derivatives of $\mathcal{V}$ with respect to any of the w_i must vanish. Between and near two identical letters, say R and R, according to Table 1, the angles are given by the table

Ω	R		R
i	0	1	2
w_i	a	b	c
x_i	$\xi - b$	$-a + 2b - c$	$-b + \xi'$
y_i	$\eta + b$	$a + c$	$b + \eta'$
z_i	$\pi - 2a$	$\pi - 2b$	$\pi - 2c$

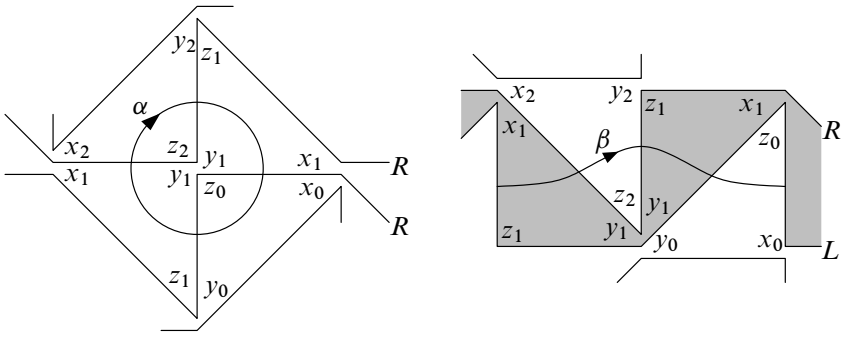

Figure 7

(the exact expression of ξ, ξ', η, η' depends on the letters before and after RR, but only the b–contribution matters here). Using Proposition 6.1, criticality of $\mathcal{V}$ implies

$$1 = \exp \frac{-\partial \mathcal{V}}{\partial b} = \frac{\sin y_0 \sin^2 x_1 \sin y_2}{\sin x_0 \sin^2 z_1 \sin x_2}.$$

Using the fact that edge lengths in a triangle are proportional to angle sines, it follows that the edge lengths in Figure 7 (left) around the central vertex fit nicely together. So $|\psi(\alpha)| = 1$. The case of a subword LL is treated similarly, which takes care of *all* 4–valent vertices of the tessellation $\mathcal{A}'$.

Near a hinge between two different letters, say L followed by R, the angles are

Ω	L		R
i	0	1	2
w_i	a	b	c
x_i	$\xi + b$	$a + b - c$	$-b + \xi'$
y_i	$\eta - b$	$-a + b + c$	$b + \eta'$
z_i	$\pi - 2a$	$\pi - 2b$	$\pi - 2c$

This time, criticality implies

$$1 = \exp \frac{-\partial \mathcal{V}}{\partial b} = \frac{\sin x_0 \sin y_1 \sin x_1 \sin y_2}{\sin y_0 \sin^2 z_1 \sin x_2}.$$

As shown in Figure 7 (right) and by the same trigonometric argument, this means that the first and last edges crossed by β have the same length. So $\psi(\beta) = 1$. (If Ω is reduced to LR, the computation is formally the same, identifying indices 0 and 2.) The case of a subword RL is similar. Sublemma 6.4 is proved. □

Now let α be an element of $\pi_1(B', x_0)$ that is conjugated to a simple loop around a 4–valent vertex of $\mathcal{A}'$. By Sublemma 6.4 (and an easy conjugation argument), $\rho(\alpha)$ is a translation. Moreover, $\rho(\alpha)$ fixes the vertex around which α revolves, so $\rho(\alpha) = 1$, the identity of the Euclidean plane.

Sublemma 6.5 *Let U be the quotient of the torus at infinity of V_φ by the action of the hyperelliptic involution σ of the fiber, so that $B' \subset U$. Suppose (w_i) is critical for $\mathcal{V}$. Then the representation $\rho\colon \pi_1(B', x_0) \to \mathbb{C}^* \ltimes \mathbb{C}$ descends to a representation $\rho_U\colon \pi_1(U, x_0) \to \mathbb{C}^* \ltimes \mathbb{C}$ whose first projection $\psi_U\colon \pi_1(U, x_0) \to \mathbb{C}^*$ is trivial.*

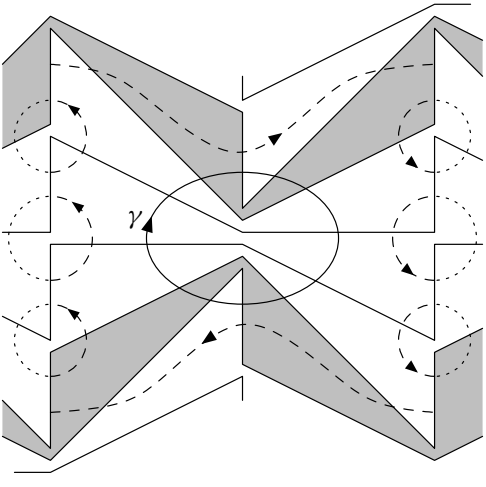

Figure 8

Proof To see that ρ_U is well-defined, we only need to check that, if γ is (conjugated to) a loop around a vertex v of $\mathcal{A}'$, then $\rho(\gamma) = 1$. If v has valence 4, it has already been done. If not, by the argument preceding Sublemma 6.5, it is sufficient to check that $\psi([\gamma]) = 1$, where $[\gamma]$ denotes the homology class of γ. But in $H_1(B', \mathbb{Z})$, the element $[\gamma]$ is a sum of loops around 4–valent vertices and curves following "grey" levels (see Figure 8: the vertical edges of B' on the two sides of the picture are identified, and the curves crossing these edges undergo a "split-and-paste" process to yield γ). So by Sublemma 6.4, $\psi([\gamma]) = 1$; therefore ρ_U is well-defined. Moreover, if β is a curve following a "grey" level, Sublemma 6.4 tells that $\rho_U(\beta) = \rho(\beta)$ is a nonidentical Euclidean *translation*. The value of ρ_U on another generator of $\pi_1(U)$ (which is abelian) must commute with $\rho_U(\beta)$, and therefore be a translation too. So ρ_U has its image contained in $\{1\} \ltimes \mathbb{C}$ and $\psi_U = 1$, completing the proof. □

By assigning length 1, for example, to the reference edge ϵ_0 of $\mathcal{A}'$, a critical point (w_i) of the volume functional thus defines the lengths of all other edges of $\mathcal{A}'$ in a coherent way. This yields a complete Euclidean metric g on U. The universal cover $\widetilde{U}$ of U thus embeds into $\mathbb{C}$ (the embedding, also called the developing map of the local Euclidean structure, can only be injective, because the $\widetilde{g}$–geodesic joining two distinct points of $\widetilde{U}$ is sent to a geodesic of $\mathbb{C}$); so there is an isometry $\widetilde{U} \simeq \mathbb{C}$. The metric g lifts from U to the torus at infinity of V_φ and its tessellation $\mathcal{A}$, producing a geometric realization of $\mathcal{A}$ and of Figure 4 in $\mathbb{C}$ (Euclidean plane tiling). Above each triangle of the universal cover of $\mathcal{A}$ now sits one ideal tetrahedron with vertex at infinity: the tetrahedron is the hyperbolic convex hull of ∞ and the vertices of the triangle. Note that these tetrahedra fill $\mathbb{H}^3$ completely above a certain height.

To make sure that the pasted metric on the union $V = V_\varphi$ of all ideal tetrahedra is now complete, assume a geodesic $\gamma(t)$ in V hits infinity at time $T < \infty$. If $K \subset V$ is compact, ie has a compact intersection with each tetrahedron Δ_i, then γ must eventually exit K (if not, the $\gamma(T - 1/n)$ accumulate at some point p of some tetrahedron, but centered at p there is a small embedded hyperbolic ball: absurd). So for t sufficiently close to T, there is a lift of $\gamma(t)$ arbitrarily high above the tessellation $\mathcal{A}$ (embedded in $\mathbb{C}$ in the upper half space model). But at sufficiently great height, the tetrahedra above $\mathcal{A}$ fill $\mathbb{H}^3$ completely, so geodesics are defined for long times (eg times larger than 1): a contradiction. The first implication of Lemma 6.2 is proved.

To prove the converse, it is enough to show that if the gluing of the tetrahedra yields a complete hyperbolic metric, then the gluing of their vertex links yields a geometric realization of $\mathcal{A}$, ie of Figure 4 (checking $\partial\mathcal{V}/\partial w_i = 0$ then amounts to a rerun of the two computations in Sublemma 6.4, distinguishing whether i is a hinge index or not). But the latter is clear: given a complete hyperbolic metric, consider a triangulated universal cover $\mathbb{H}^3 \to V_\varphi$ and send (a lift of) the cusp to infinity in the upper half space model. It is a classic argument that deck transformations of $\mathbb{H}^3$ which fix infinity must be parabolic, so the link of infinity has two translational periods and provides a Euclidean realization of $\mathcal{A}$ (and of Figure 4). □

6.3 Behavior of the volume functional

As a consequence of Lemma 6.2, to prove Theorem 1.1 we only need to find a critical point of the volume functional $\mathcal{V}$ in the open polyhedron P of cyclic sequences (w_i) satisfying the conditions (3). A few more facts about the volume of ideal hyperbolic tetrahedra will be needed.

By Proposition 6.1, the volume functional $\mathcal{V}$ continuously extends to the (compact) closure $\overline{P}$ of the polyhedron P (the space $\overline{P}$ is defined by turning the conditions

(3) to weak inequalities, or taking the limits in $\mathbb{R}^m$ of sequences of P). Then $\mathcal{V}$ has well-defined extrema on $\bar{P}$, which are automatically critical if they belong to P. Because of the following proposition, the only possibility for a critical point is to be an absolute maximum.

Proposition 6.6 *The volume of an ideal tetrahedron is a concave function of its dihedral angles.*

Proof This follows from Proposition 6.1, whose notations we use again: x_t, y_t, z_t are the dihedral angles. By symmetry we may assume $x_0, y_0 \leq \pi/2$. Assume further that x_t, y_t, z_t are affine functions of t with first-degree coefficients X, Y, Z. Proposition 6.1 implies $-d\mathcal{V}/dt = X \log\sin x_t + Y \log\sin y_t + Z \log\sin z_t$, and by differentiating we obtain

$$\begin{aligned}
-d^2\mathcal{V}/dt^2|_{t=0} &= X^2 \cot x_0 + Y^2 \cot y_0 + Z^2 \cot z_0 \\
&= X^2 \cot x_0 + Y^2 \cot y_0 + (X+Y)^2 \frac{1 - \cot x_0 \cot y_0}{\cot x_0 + \cot y_0} \\
&= \frac{(X+Y)^2 + (X \cot x_0 - Y \cot y_0)^2}{\cot x_0 + \cot y_0} \geq 0. \qquad \square
\end{aligned}$$

As a consequence, the volume functional $\mathcal{V}$ is also concave on $\bar{P}$ and Theorem 1.1 holds if the maximum of $\mathcal{V}$ is interior. Next we explore the behavior of $\mathcal{V}$ near the boundary of $\bar{P}$.

Proposition 6.7 (Simple degeneracy) *If $(Q_t)_{t\geq 0}$ is a smooth family of ideal tetrahedra with dihedral angles x_t, y_t, z_t such that $x_0, y_0 \in (0,\pi)$; $z_0 = 0$ and $\frac{dz_t}{dt}|_{t=0} > 0$, then $\frac{d\mathcal{V}}{dt}|_{t=0} = +\infty$.*

Proof Simply check that the right hand side of (5) goes to 0 as t goes to 0. We call this situation *simple degeneracy* because the limiting triangle has only one vanishing angle (two of its vertices are therefore collapsed). $\square$

Proposition 6.8 (Double degeneracy) *If $(Q_t)_{t\geq 0}$ is a smooth family of ideal tetrahedra satisfying $(x_0, y_0, z_0) = (0, 0, \pi)$ and $\frac{d}{dt}|_{t=0}(x_t, y_t, z_t) = (1+\lambda, 1-\lambda, -2)$ with $\lambda \in (-1, 1)$, then*

$$\exp \frac{-d\mathcal{V}}{dt}\Big|_{t=0} = \frac{1-\lambda^2}{4} \left(\frac{1+\lambda}{1-\lambda}\right)^{\lambda}.$$

Proof As t goes to 0, one has $\sin x_t \sim (1+\lambda)t$ and $\sin y_t \sim (1-\lambda)t$ and $\sin z_t \sim 2t$. The right hand side of (5) is thus equivalent to

$$\big((1+\lambda)t\big)^{1+\lambda}\big((1-\lambda)t\big)^{1-\lambda}(2t)^{-2} = \frac{1-\lambda^2}{4}\left(\frac{1+\lambda}{1-\lambda}\right)^{\lambda}.$$

We call this situation *double degeneracy* because the limiting triangle has two vanishing angles (its vertices are distinct, but collinear). At a double degeneracy, the volume has directional derivatives, but no well-defined differential. □

7 Ruling out some degeneracies

From now on, we fix (w_i) in the compact polyhedron $\overline{P}$ at a point which maximizes the total hyperbolic volume of all tetrahedra. To prove that (w_i) is critical for the volume $\mathcal{V}$, we only need to make sure that (w_i) lies in the interior P of $\overline{P}$, ie that all x_i, y_i, z_i lie in $(0,\pi)$.

Proposition 7.1 *If for some index i, one of the numbers x_i, y_i, z_i is 0, then two of them are 0 and the third is π. In other words, there are no simple degeneracies, only double degeneracies.*

Proof If not, consider an affine segment from (w_i) to some interior point of P. By Proposition 6.7, the partial derivative of $\mathcal{V}$ at (w_i) along that segment is not bounded above, so $\mathcal{V}$ was not maximal at (w_i). □

Tetrahedra Δ_i such that (x_i, y_i, z_i) has one, and therefore two vanishing terms are called *flat*, and are characterized by the property that w_i is either 0 or $\frac{\pi}{2}$.

Proposition 7.2 (Domino effect) *If two consecutive tetrahedra Δ_{i-1}, Δ_i are flat, then Δ_{i+1} is flat, too.*

Proof We use only Table 1 and the deductions recorded in (3). There are three cases:

(1) If i is not a hinge index, flatness of Δ_i implies $w_{i-1} + w_{i+1} \in \{0, \pi\}$. By the range condition $0 \le w \le \frac{\pi}{2}$, this implies $w_{i+1} \in \{0, \frac{\pi}{2}\}$, so Δ_{i+1} is flat.

(2) If i is a hinge index and $w_i = \frac{\pi}{2}$, we must have $|w_{i-1} - w_{i+1}| = \frac{\pi}{2}$, so by the range condition, w_{i+1} is 0 or $\frac{\pi}{2}$, and Δ_{i+1} is flat.

(3) If i is a hinge index and $w_i = 0$, we have $|w_{i+1} - w_{i-1}| \le 0$ so $w_{i+1} = w_{i-1}$. But Δ_{i-1} is assumed flat, and therefore so is Δ_{i+1}. Note that flatness of Δ_{i-1} was needed only in this case. □

Proposition 7.3 *If Δ_i is flat, then i is a hinge index and $w_i = 0$.*

Proof In all other cases, the proof of Proposition 7.2 actually forces Δ_{i+1} to be flat, which triggers a domino effect: all Δ_j's are flat, and the volume is 0 — certainly not maximal. □

Easy Fact 7.4 If ABC is a Euclidean triangle with positive angles and edge lengths a, b, c, then

$$a = b \iff \widehat{A} = \widehat{B} \iff \sin\widehat{A} = \sin\widehat{B}$$
$$a < b \iff \widehat{A} < \widehat{B} \iff \sin\widehat{A} < \sin\widehat{B}.$$

The volume $\mathcal{V}$ is still supposed maximal, and we assume that some tetrahedra Δ_i are flat, ie that some hinge parameters w_i vanish. Places where a parameter w_i vanishes will be signalled by a vertical bar: $\dots LL|RR\dots$ By Proposition 7.2, consecutive vertical bars are always separated by at least two letters.

The patterns $RL|RL$ and $LR|LR$ can never occur, because increasing the incriminated w_i to ε would automatically increase the volume (note that $w_{i-1} = w_{i+1} =: A$ by the hinge condition (3)-iii):

Ω	L		R	$\vert$	L		R	
w_i	u	A		$0+\varepsilon$		A		v
x_i	.	$u+A-\varepsilon$		ε		$\varepsilon+A-v$		.
y_i	.	$-u+A+\varepsilon$		ε		$-\varepsilon+A+v$		.
z_i	.	$\pi-2A$		$\pi-2\varepsilon$		$\pi-2A$		.

This implies

$$\exp\frac{-\partial\mathcal{V}}{\partial\varepsilon}\Big|_{\varepsilon=0} = \frac{1}{4}\cdot\frac{\sin(A-u)}{\sin(A+u)}\frac{\sin(A-v)}{\sin(A+v)} < 1$$

where we used Easy Fact 7.4, Proposition 6.1 and Proposition 6.8 (with $\lambda = 0$).

Any vertical bar thus lives next to at least two consecutive identical letters (on at least one side). However, the patterns $R|LL|R$ and $L|RR|L$ are also prohibited by Proposition 7.3, since the central (nonhinge) tetrahedron would have one vanishing angle ($a + c = 0$ in the notations of Table 1).

8 A geometrical lemma

Definition 8.1 In the universal cover of the tessellation $\mathcal{A}$ of the torus at infinity of V_φ (Figure 4), a *fan* is a sequence of at least three consecutive layers, such that the first and last layers are grey and all layers in between are white. Fans are in bijection

with the subwords of Ω of the form RL^kR or LR^kL with $k \geq 2$ (see the remarks to Figure 4 in Section 4).

Lemma 8.2 *Suppose $w_0 = 0$, so that Ω contains a subword $L|R^kL$ with $k \geq 2$, or $L|R^k|L$ with $k \geq 3$ (in the latter case, the second bar indicates that w_k vanishes as well as w_0). The corresponding fan admits a complete Euclidean structure with boundary (with angles prescribed by the w_i's). Moreover, let Q, P, T be the lengths of the segments of the broken line corresponding to the first R, in the order indicated in Figure 9 (P, T are the sides adjacent to the apex in a flat upward-pointing grey [hinge] triangle, in the sense of Figure 3). Then $Q < P + T$.*

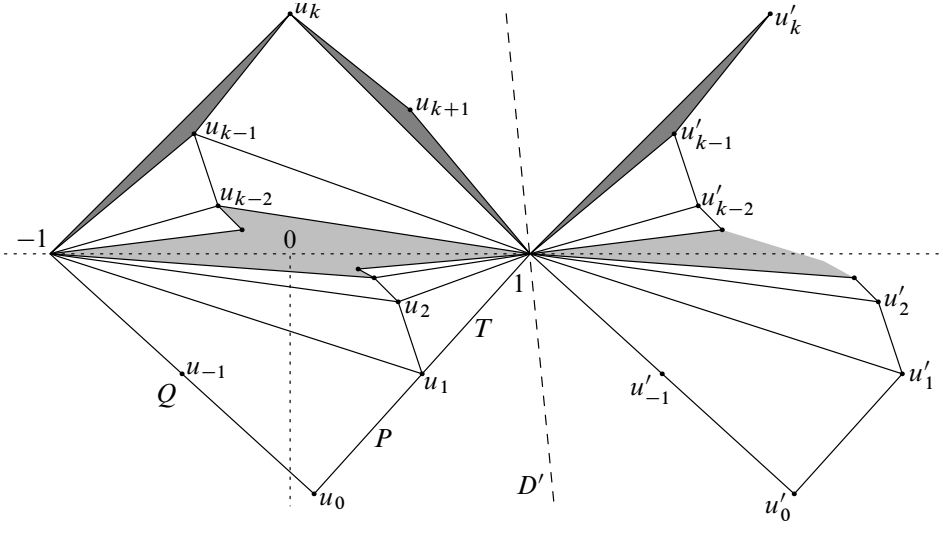

Figure 9: The situation where $Q \geq P + T$ cannot hold

Proof We first restrict our attention to the case $L|R^kL$, $k \geq 2$. The interior vertices of the topological fan correspond to the indices i living between two R's, ie $1 \leq i \leq k-1$, in the sense that holonomy around the i–th vertex u_i (Figure 9) is controlled by $\partial\mathcal{V}/\partial w_i$ (Sublemma 6.4). When $2 \leq i \leq k-1$, none of the triangles adjacent to u_i are flat, so w_i can vary in a small interval without making the m–tuple w exit the domain $\overline{P}$; consequently, the value of w_i in that interval is critical, which by the first case (nonhinge) of Sublemma 6.4 implies that the holonomy around the associated vertex u_i is trivial. As for $i = 1$, the corresponding vertex u_1 is adjacent to a flat angle $z_0 = \pi$ (Figure 9) so its holonomy is not imposed by the w_i's (when a triangle has an angle π, the other two angles are always 0 while the adjacent sides may have arbitrary lengths).

The case of $L|R^k|L$ is similar: for indices $2 \le i \le k-2$, Sublemma 6.4 applies, while for $i = 1$ or $k-1$ holonomy is not imposed by the w_i's.

Therefore we can embed the fan as an infinite necklace of triangulated polygons into $\mathbb{C}$. We shall no longer distinguish $L|R^kL$ from $L|R^k|L$ here, and shall formulate all properties in terms of complex numbers in order to keep track of *oriented* angles. We make two consecutive nodes (ie lifts of the $(2k+4)$–valent vertex of $\mathcal{A}$ associated to the full subword LR^kL) coincide with -1 and 1 in $\mathbb{C}$, and also denote by u_i the complex coordinate of the copy of u_i between these nodes (the index i actually ranges from -1 to $k+1$; see Figure 9). Incidentally, one can show that the u_i form (part of) an orbit of a certain deck transformation of the universal cover $\mathbb{H}^3 \to V_\varphi$. We will discuss this more at the end of Section 10.

We arrange matters so that $\mathrm{Im}(u_0) < 0$ and u_1 lies on the open segment $(u_0, 1)$. While removing any node disconnects the fan, Condition (1)-iii implies that the image of the embedding is invariant under a horizontal translation of length 2. In particular, the geometric link of each node, such as 1 or -1, is completely determined. To prove the assertion of the Lemma, it is sufficient to show that $\mathrm{Re}(u_0) < 0$. Assume $\mathrm{Re}(u_0) \ge 0$ (so u_0 lies in the lower-right quadrant) and aim for a contradiction.

The similarity property of the triangles with vertices $1, u_i, u_{i+1}$ and $-1, u_i, u_{i-1}$ is expressed by the relation $\frac{u_{i+1}-1}{u_i-1} = \frac{u_{i-1}+1}{u_i+1}$, hence by induction

$$(u_{i+1}-1)(u_i+1) = (u_i-1)(u_{i-1}+1) = \cdots = (u_1-1)(u_0+1) =: K.$$

Then, as u_1 sits between 1 and u_0, the number $u_1 - 1$ is a positive (real) multiple of $u_0 - 1$, so K is a positive multiple of $u_0^2 - 1$ which implies $\mathrm{Im}(K) \le 0$. Let D be the line through 0 and the points $\pm\sqrt{K}$: either D is vertical, or D visits the upper-left and lower-right (open) quadrants. Let D' be the line through 1, parallel to D; and define $u_i' := 2 + u_i$ for all i. By definition of K, the rays $[1, u_{i+1})$ and $[1, u_i')$ are symmetric with respect to D'. Moreover, the rays through $u_0, u_1, \ldots, u_k, u_{k+1}, u_k', u_{k-1}', \ldots, u_0', u_{-1}', u_0$ issuing from 1 (in that cyclic order) divide $\mathbb{C}$ into angular sectors of sum 2π realizing the geometric link of a node of the fan, as specified by the angles $x_i, y_i, z_i \ge 0$. Finally, since all these angles are nonnegative, the symmetry of the link with respect to D' implies that for all $-1 \le i \le k$, the point u_i' (resp. u_{i+1}) is on the right (resp. left) of D'.

Recall $\mathrm{Im}(u_0) < 0$. Suppose by induction $\mathrm{Im}(u_i) < 0$ for some $0 \le i \le k$. Then $\mathrm{Im}(u_i') < 0$. Considering the direction of D' and the symmetry property with respect to D', this implies $\mathrm{Im}(u_{i+1}) < 0$. By an immediate induction, the angular sector $\widehat{u_{k+1}\,1\,u_k'}$ (just above 1) is larger than π. But it is an angle of the link at the node 1 (namely, z_{k+1}), giving a contradiction. □

Of course, a statement similar to Lemma 8.2 holds for subwords $LR^k|L$, and also for $R|L^kR$, $R|L^k|R$ and $RL^k|R$.

9 Ruling out all degeneracies

Easy Fact 9.1 If U and V are positive constants, the function defined on $(-1,1)$ by

$$f(\lambda) := \frac{1-\lambda^2}{4} U\left(\frac{1+\lambda}{1-\lambda} V\right)^{\lambda}$$

takes the value $\frac{U}{(1+V)(1+V^{-1})}$ for some λ. It is in fact an absolute minimum: indeed,

$$(\log f)'(\lambda) = \log\left[\frac{1+\lambda}{1-\lambda} V\right],$$

so f is minimal when the bracket is 1, and the result follows by direct computation.

Now we can prove that the configuration $\dots RR|L\dots$ (and similarly $\dots LL|R\dots$) never occurs, which will imply Theorem 1.1. The strategy is to suppose $RR|L$ appears, ie $w_j = 0$ for some j (for notational convenience we assume $j = 2$). Next, replace w_2 by ε and w_1 by $w_1 + \lambda\varepsilon$, for a wisely chosen λ. The volume $\mathcal{V}$ will then increase. (The value of λ, which does not need to be explicitly computed, will maximize $\partial\mathcal{V}/\partial\varepsilon$, and $e^{-\partial\mathcal{V}/\partial\varepsilon}$ will be the value of f given in Easy Fact 9.1. We will specify in due time what the parameters U, V are.) Volume computations follow from Proposition 6.8 (at the index $i = 2$) and Proposition 6.1 (other indices).

9.1 Case 1: $RR|LR$

According to Table 1, the angles are as follows. Note the relation $w_1 = w_3 =: A$, a consequence of the hinge condition (3)-iii.

Ω	R	R	$\|$	L	R
i	0	1	2	3	4
w_i	u	$A+\lambda\varepsilon$	$0+\varepsilon$	A	v
x_i	$\xi - A - \lambda\varepsilon$	$-u+2A+2\lambda\varepsilon-\varepsilon$	$(1-\lambda)\varepsilon$	$\varepsilon+A-v$	.
y_i	$\eta + A + \lambda\varepsilon$	$u+\varepsilon$	$(1+\lambda)\varepsilon$	$-\varepsilon+A+v$	.
z_i	$\pi - 2u$	$\pi - 2A - 2\lambda\varepsilon$	$\pi - 2\varepsilon$	$\pi - 2A$	.

We have $u = w_0 > 0$ because $L|RR|LR$ is impossible (according to the discussion after Easy Fact 7.4). Thus, Δ_0 is not flat: if $-1 < \lambda < 1$, then ε can take small positive

values without making any of the x_i, y_i, z_i negative. With the correct choice of λ, we deduce

$$\exp \frac{-\partial \mathcal{V}}{\partial \varepsilon}\Big|_{\varepsilon=0} = \frac{1-\lambda^2}{4} \overbrace{\underbrace{\frac{\sin(A-v)}{\sin(A+v)}}_{\leq 1} \underbrace{\frac{\sin y_1}{\sin x_1}}_{Q/P}}^{U} \left(\frac{1+\lambda}{1-\lambda} \underbrace{\frac{\sin y_0 \sin^2 x_1}{\sin x_0 \sin^2 z_1}}_{P/T=:V} \right)^{\lambda}$$
$$\leq \frac{Q/P}{(1+P/T)(1+T/P)} = \frac{1}{1+P/T} \frac{Q}{P+T} < 1$$

by Lemma 8.2 (see Figure 10 (left) — again, the sine relation in triangles was used to compute Q/P and P/T).

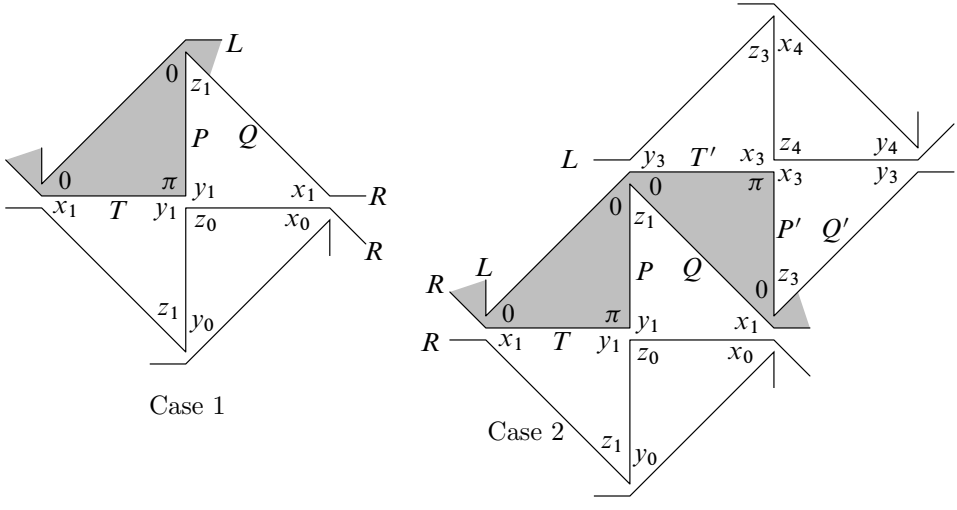

Figure 10

9.2 Case 2: $RR|LL$

Ω	R		R | L		L
i	0	1	2	3	4
w_i	u	$A+\lambda\varepsilon$	$0+\varepsilon$	A	v
x_i	$\xi - A - \lambda\varepsilon$	$-u+2A+2\lambda\varepsilon-\varepsilon$	$(1-\lambda)\varepsilon$	$\varepsilon+v$	$A+\xi'$
y_i	$\eta + A + \lambda\varepsilon$	$u+\varepsilon$	$(1+\lambda)\varepsilon$	$-\varepsilon+2A-v$	$-A+\eta'$
z_i	$\pi - 2u$	$\pi - 2A - 2\lambda\varepsilon$	$\pi - 2\varepsilon$	$\pi - 2A$	$\pi - 2v$

First consider the value of A. Since there can be no vertical bars immediately before or after $RR|LL$, the tetrahedra $\Delta_0, \Delta_1, \Delta_3, \Delta_4$ have positive angles, so the parameter

A (which does not contribute to the angles of any other tetrahedra) can vary freely in an open interval when $\varepsilon = 0$. So A must be critical giving

$$1 = \exp \frac{-\partial \mathcal{V}}{\partial A}\Big|_{\varepsilon=0} = \underbrace{\frac{\sin y_0 \sin^2 x_1}{\sin x_0 \sin^2 z_1}}_{P/T} \underbrace{\frac{\sin^2 y_3 \sin x_4}{\sin^2 z_3 \sin y_4}}_{P'/T'}.$$

Hence $P/T = T'/P'$. Therefore, with the right choice of λ,

$$\begin{aligned}\exp \frac{-\partial \mathcal{V}}{\partial \varepsilon}\Big|_{\varepsilon=0} &= \frac{1-\lambda^2}{4} \overbrace{\underbrace{\frac{\sin y_1}{\sin x_1}}_{Q/P} \underbrace{\frac{\sin x_3}{\sin y_3}}_{Q'/P'}}^{U} \left(\frac{1+\lambda}{1-\lambda} \underbrace{\frac{\sin y_0 \sin^2 x_1}{\sin x_0 \sin^2 z_1}}_{P/T=T'/P'=:V} \right)^{\lambda} \\ &= \frac{Q/P \cdot Q'/P'}{(1+T/P)(1+T'/P')} = \frac{Q}{P+T} \frac{Q'}{P'+T'} < 1\end{aligned}$$

by Lemma 8.2; see Figure 10 (right).

We conclude with two remarks. First, up to replacing the monodromy φ with φ^2 (thus doubling the period m of Ω), we can always assume Ω has at least 6 letters: that way, all columns of the tables above are neatly distinct, and to recover the original V_φ we just quotient out by the extra symmetry (which the volume maximizer $(w_i)_{i\in\mathbb{Z}/m\mathbb{Z}}$ must respect, by concavity of the volume functional $\mathcal{V}$). Compare with the remark that closes Section 5. Second, the choice of $\lambda \in (-1, 1)$, which may seem "magical" at first glance, is essentially our only degree of freedom in Section 9.1–Section 9.2: the volume is already assumed critical with respect to most parameters (including A, the common value of w_1 and w_3); therefore, only deformations of w_1, w_2, w_3 need to be considered, and if we assume $\frac{\partial w_2}{\partial \varepsilon} = 1$, then only the value of the difference $\frac{\partial w_1}{\partial \varepsilon} - \frac{\partial w_3}{\partial \varepsilon} \in (-1, 1)$ matters.

Theorem 1.1 is proved.

10 A numerical example: $R^N L^M$

In this section we fix two large enough integers N and M and investigate the behavior of the angles for $\Omega = R^N L^M$: the angles made positive by the previous computations will turn out to be very small. We will directly construct a Euclidean realization of Figure 4, automatically unique up to isometry. Since N and M are large, there exist small complex numbers a, a', b, b' such that

$$(6) \qquad \begin{cases} \sin a &= i \tan b \cos b' \\ \sin a' &= -i \tan b' \cos b \end{cases} \quad \text{where} \quad \begin{cases} b &= (\pi - 2a)/N \\ b' &= (\pi - 2a')/M. \end{cases}$$

A way to compute a, a' is to set $a_0 = a'_0 = 0$ and to define inductively

$$a_{s+1} = \arcsin\left(i \tan\frac{\pi - 2a_s}{N} \cos\frac{\pi - 2a'_s}{M}\right)$$

and a similar expression for a'_{s+1}, with a change of sign. The sequences a_s, a'_s converge exponentially fast to a, a'. The constants a, a' become arbitrarily small for large enough N, M, hence $b \sim \pi/N$ and $b' \sim \pi/M$. So plugging into (6), $a \sim i\pi/N$ and $a' \sim -i\pi/M$. Using the Landau symbol $O(A, B)$ in the sense of $O(\max\{A, B\})$, this in turn yields

$$\begin{aligned} b &= \tfrac{\pi}{N} - \tfrac{2i\pi}{N^2} + O\left(\tfrac{1}{N^3}, \tfrac{1}{M^3}\right) & a &= \tfrac{i\pi}{N} + \tfrac{2\pi}{N^2} + O\left(\tfrac{1}{N^3}, \tfrac{1}{M^3}\right) \\ b' &= \tfrac{\pi}{M} + \tfrac{2i\pi}{M^2} + O\left(\tfrac{1}{N^3}, \tfrac{1}{M^3}\right) & a' &= \tfrac{-i\pi}{M} + \tfrac{2\pi}{M^2} + O\left(\tfrac{1}{N^3}, \tfrac{1}{M^3}\right). \end{aligned} \tag{7}$$

(In fact a, a', b, b' are analytic functions of $\frac{1}{N}, \frac{1}{M}$, by the Implicit Function Theorem.)

Proposition 10.1 *The fan which corresponds to R^N can be embedded into $\mathbb{C}$ with nodes at complex coordinates $\pm\cot b$ and intermediary vertices $\cot(a + sb)$ where $-1 \le s \le N + 1$; similarly, the fan corresponding to L^M can be embedded into $\mathbb{C}$ (possibly with a different scaling factor) with nodes $\pm\cot b'$ and intermediary vertices $\cot(a' + sb')$ where $-1 \le s \le M + 1$ (see Figure 11).*

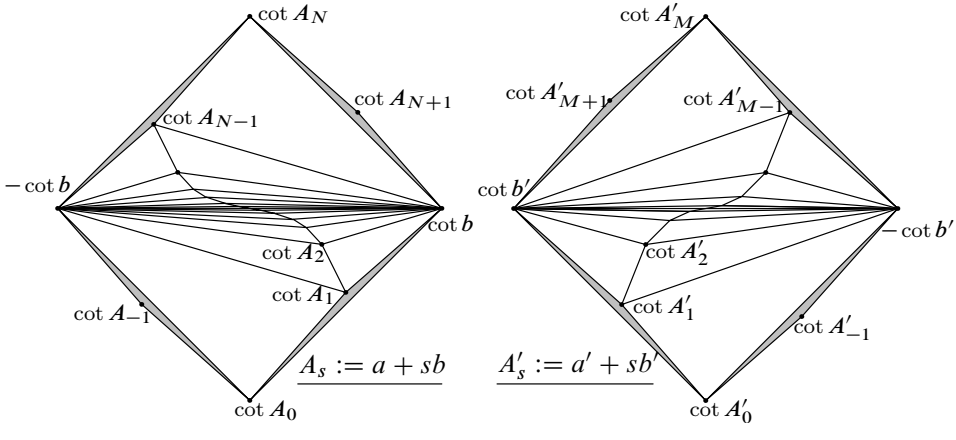

Figure 11

Proof There are several things to check. First, the congruence of pairs of triangles inside each fan follows from the identity of complex ratios

$$\frac{\cot(A_s+b)-\cot b}{\cot(A_s+b)-\cot A_s}=\frac{\cot(A_s-b)+\cot b}{\cot(A_s-b)-\cot A_s}=\frac{\sin^2 A_s}{\sin^2 b} \tag{8}$$

where $A_s=a+sb$ for $0\le s\le N$, and an identical relation for a',b'.

Next, each fan, when stripped of two of its four limiting (grey) triangles, is a parallelogram. This follows from $\cot(a+Nb)=\cot(\pi-a)=-\cot a$, and the same for a'. In particular, each fan admits a center of symmetry.

Furthermore, these two parallelograms are congruent. To see this, let $\alpha,\alpha',\beta,\beta'$ denote the *squared cotangents* of a,a',b,b'. Raising (6) to the power -2, we get

$$\begin{cases} 1+\alpha &= -\beta(1+\beta'^{-1}) \\ 1+\alpha' &= -\beta'(1+\beta^{-1}) \end{cases} \quad \text{hence} \quad \frac{\alpha}{\alpha'}=\frac{\beta+\beta/\beta'+1}{\beta'+\beta'/\beta+1}=\frac{\beta}{\beta'},$$

so $\cot a/\cot b=\pm\cot a'/\cot b'$, the correct sign being minus by the estimates (7).

Further yet, the limiting (grey) triangles of the two fans have the same shape: by (8) their complex ratios are $\sin^2 a/\sin^2 b$ and $\sin^2 b'/\sin^2 a'$, both equal by (6) to $-\cos^2 b'/\cos^2 b$.

Finally, all triangles are positively oriented, that is, $\operatorname{Im}(\sin^2 A_s/\sin^2 b)>0$ for all $0\le s\le N$. We first check this for $s=0$ (the case $s=N$ will follow by symmetry): we have $\sin^2 a/\sin^2 b=-(\cos^2 b'/\cos^2 b)=-((1-\sin^2 b')/(1-\sin^2 b))$. In the latter expression, both the numerator and denominator are ~ 1, but their imaginary parts are equivalent to $-4\pi^2/M^3$ and $4\pi^2/N^3$ respectively (with an $O(N^{-4},M^{-4})$ error), by (7). Therefore, the ratio does lie above the real line, and the "pinched" angles of the limiting (grey) triangles in Figure 11 are both roughly

$$2\pi^2(N^{-3}+M^{-3}) \text{ radians.}$$

Very pinched, but not flat!

To check that $\arg(\sin A_s/\sin b)$ lies in $(0,\pi/2)$ for all other $0\le s\le N$, we need to draw the level curves of $z\mapsto\arg(\sin z)$ in $\mathbb{C}$. This is done in Figure 12, in the case $0\le\operatorname{Re}(z)\le\pi$: the curves fall into 4 symmetric families ("quadrants" meeting at $\pi/2\in\mathbb{C}$), and it is an easy exercise to check that the families above (resp. below) the real axis are made of convex (resp. concave) curves. The authorized region for the $A_s=a+sb$ is in grey (with a narrow collar near $\pi/2$); the forbidden regions are left in white. The segment $[A_0A_N]$ clearly stays in the grey region, which implies the result.

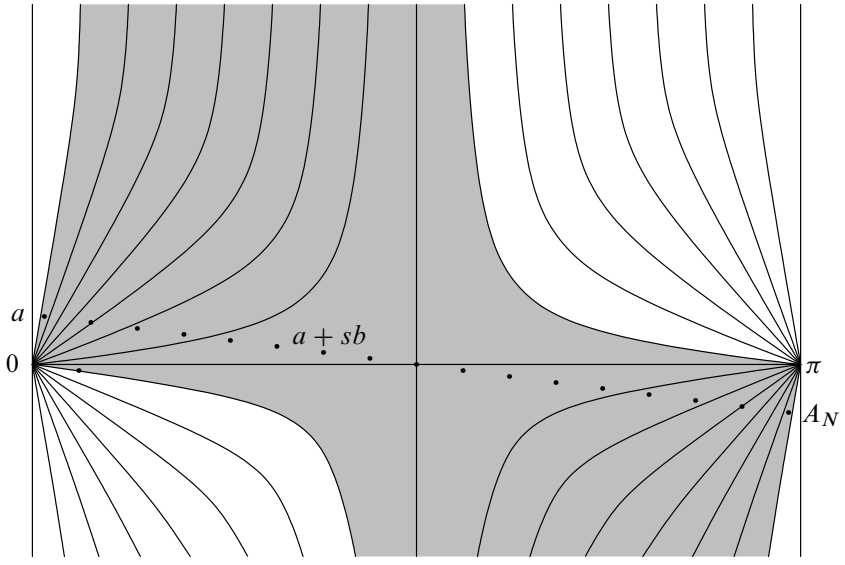

Figure 12: Level curves of $z \mapsto \arg(\sin z)$

By the same argument, the triangles in the fan of L^M are well-oriented, too. Therefore we may tile the plane with parallelograms (or fans) congruent to those in Figure 11 to get a Euclidean realization of Figure 4. □

Finally, notice that the Kleinian group associated to the embedding of the left fan in Figure 11 contains the Möbius transformation $z \mapsto (z\cos b - \sin b/(z\sin b + \cos b))$ (it sends each tetrahedron sitting above a triangle in the left half of the fan to the tetrahedron sitting above the similar triangle in the right half). Therefore, $2ib$ (and similarly $-2ib'$) are the complex lengths of very short closed geodesics in the hyperbolic manifold V_φ.

A consequence of Theorem 1.1 is that the volume of any angle structure (defined by Table 1, where (3) holds) is a lower bound for the volume of the manifold V_φ. One gets bounds which are sharp in terms of distances in the Farey graph; see Section B.1.

11 Once-punctured tori and 4–punctured spheres

Theorem 1.1 is still true if we replace the once-punctured torus T by the 4–punctured sphere S, and the map $\varphi\colon T \to T$ by an orientation-preserving homeomorphism $\varphi_S\colon S \to S$ (of course, we must specify how the "eigenvalues" of φ_S are defined). In fact, the tetrahedra of the resulting manifold V_{φ_S} and of V_φ are metrically the same; only the combinatorics of their gluing changes a little.

Define $R := \mathbb{R}^2 \smallsetminus \mathbb{Z}^2$ and the maps $\alpha, \beta, \sigma\colon R \to R$ characterized by $\alpha(x) = x + (1,0)$; $\beta(x) = x + (0,1)$; $\sigma(x) = -x$. Then we have natural identifications $T = R/\langle \alpha, \beta \rangle$ and $S = R/\langle \alpha^2, \beta^2, \sigma \rangle$. Define also $T' := R/\langle \alpha^2, \beta^2 \rangle$ (note that T' is a 4–punctured torus).

One can show that up to isotopy, any orientation-preserving diffeomorphism φ_S of S lifts to a map $\varphi_R\colon R \to R$ such that $\varphi_R(x) = Mx + v$ for some $M \in \mathrm{SL}_2(\mathbb{Z})$ and $v \in \mathbb{Z}^2$. Moreover, $(\pm M)$ and $(v \bmod 2\mathbb{Z}^2)$ are unique. So we may define the eigenvalues of φ_S (up to sign) as those of M. Observe finally that φ_R induces orientation-preserving diffeomorphisms $\varphi'\colon T' \to T'$ and $\varphi_T\colon T \to T$.

There are obvious coverings $T' \to T$ and $T' \to S$, of degrees 4 and 2 respectively. Given an ideal triangulation τ_T of T (corresponding to a Farey triangle), we can lift τ_T to an ideal triangulation τ' of T'. Observe that σ acts on T' as a properly discontinuous involution fixing τ', hence τ' descends to a triangulation τ_S of S. It is easy to see that τ_S has the combinatorics of a tetrahedron. If τ_T and τ_T^1 are separated by a diagonal exchange (see Section 3.1 for a definition), then τ_S and the corresponding τ_S^1 are separated by two diagonal exchanges on opposite edges. Mutatis mutandis, the construction of Section 3 provides ideal (topological) triangulations of $T' \times \mathbb{R}$ and $S \times \mathbb{R}$, as well as of their quotients $V_{\varphi'}$ and V_{φ_S}. There are coverings $V_{\varphi'} \to V_{\varphi_S}$ and $V_{\varphi'} \to V_{\varphi_T}$ (of degrees 2 and 4 respectively), and all these manifolds are hyperbolic when φ_S has distinct real eigenvalues.

Appendix A Geometric triangulations of two-bridge link complements

DAVID FUTER

This appendix applies Guéritaud's techniques to find geometric triangulations for the hyperbolic two-bridge knot and link complements. These ideal triangulations are, in essence, the monodromy triangulations of 4–punctured sphere bundles, closed off in a slightly different way. They were constructed and studied in great detail by Sakuma and Weeks [23]. Akiyoshi, Sakuma, Wada and Yamashita have announced a proof that these triangulations are, in fact, geometrically canonical [5], which is a stronger statement than our result.

We will begin by reviewing two-bridge links and these ideal triangulations. We will then explain how the methods of the preceding paper give linear angle structures for these triangulations and prove that the volume function is maximized in the interior of the space of angle structures. Finally, we will prove two corollaries of this argument: a two-sided bound on the volume of the link complement and a result about arcs in the plane being hyperbolic geodesics.

A.1 Braids and two-bridge links

Let S be a 4–punctured sphere, visualized concretely as a square pillowcase with the corners removed. A 4–string braid between two pillowcases, one interior and one exterior, defines a so-called *product region* $S \times I$. We will restrict our attention to alternating braids in which the top right strand is free of crossings. (See Figure 13 (a).)

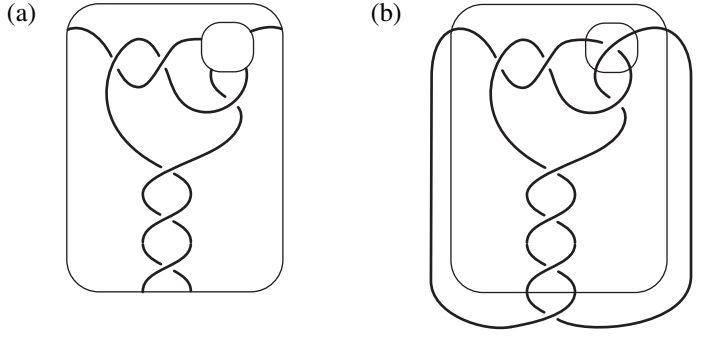

Figure 13: (a) An alternating braid between two pillowcases, described by the word $\Omega = R^3 L^2 R$ (b) The corresponding two-bridge link $K(\Omega)$

The mapping class $\varphi\colon S \to S$ induced by this braid can be described by a word

$$\Omega := \begin{cases} R^{a_1} L^{a_2} \cdots R^{a_n} \quad \text{or} \quad L^{a_1} R^{a_2} \cdots L^{a_n} & \text{with odd } n, \text{ or} \\ R^{a_1} L^{a_2} \cdots L^{a_n} \quad \text{or} \quad L^{a_1} R^{a_2} \cdots R^{a_n} & \text{with even } n. \end{cases}$$

Here, R encodes a crossing on the bottom pair of strands, and L encodes a crossing on the left pair of strands, as in Figure 14. Each *syllable* of Ω (that is, each maximal subword R^{a_i} or L^{a_i}) corresponds to a *twist region* in which two strands of the braid wrap around each other a_i times. As we read Ω from left to right, we scan the crossings from the outside in. Note that, unlike the case of punctured torus bundles, our word Ω has a beginning and an end. For concreteness, we will focus on the case when Ω starts with R, as in Figure 13 (a); the L–case is similar.

An alternating braid of this sort can be completed to a link diagram, as follows. Outside the outer pillowcase, we connect the bottom left strand to the top right, and the bottom right strand to the top left, adding an extra crossing. (Up to isotopy of $\mathbb{S}^2$, there is a unique way to do this while keeping an alternating projection. In Figure 13 (b), the extra crossing was arbitrarily placed at the bottom of the diagram.) Similarly, inside the inner pillowcase we connect the strands in a diagonal fashion, adding an extra crossing while preserving the alternating projection. This creates an alternating link $K(\Omega)$, as in Figure 13 (b).

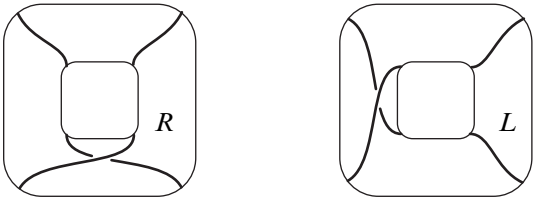

Figure 14: The letters R and L acting on strands of a braid

K is called a *two-bridge link* because this diagram can be isotoped so that the pillowcases are horizontal, and the connecting strands form two bridges between the strands of the braid. It is well-known that, apart from the trivial link of one or two components, every two-bridge link can be constructed in this way. (See, for example, Murasugi [19, Theorems 9.3.1 and 9.3.2].)

William Menasco's theorem about hyperbolic alternating links [15] contains the following special case.

Theorem A.1 *The two-bridge link $K(\Omega)$ is hyperbolic if and only if Ω has two or more syllables.*

Just as with punctured torus bundles, we will give a direct proof of the "if" direction of this theorem by finding a geometric ideal triangulation of the link complement. The "only if" direction is immediate: a word with a single syllable produces a link with a single twist region, which must be a torus link.

A.2 The ideal triangulation

The word Ω describes a monodromy triangulation of the product region $S\times I$, in exactly the same fashion as for 4–punctured sphere bundles. In fact, because this product region is the complement of a braid in the part of $\mathbb{S}^3$ bounded by the two pillowcases, we can locate the edges of the triangulation concretely in the projection diagram.

Let $c=\sum_{i=1}^{n} a_i$ be the length of Ω. Each letter Ω_i $(1\le i\le c)$, and thus each crossing in the alternating braid, corresponds to a 4–punctured sphere $S_i\subset \mathbb{S}^3\smallsetminus K$, with the four strands of K seen in Figure 14 passing through the four punctures. The braid induces an ideal triangulation on each S_i, whose edges come from arcs in the diagram that look vertical and horizontal immediately before and/or after the corresponding crossing. See Figure 15.

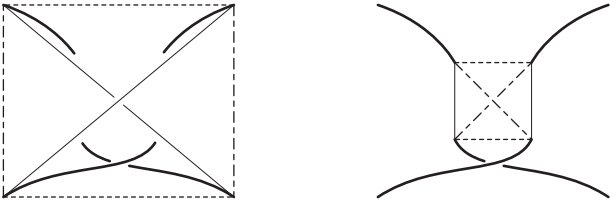

Figure 15: Two views of the same 4–punctured sphere S_i living near a crossing in the link diagram (arcs with the same dashing pattern have the same slope)

Just as with punctured torus bundles, we can locate the progressively changing triangulations in the Farey tesselation F. Each triangulation of a 4–punctured sphere S_i, containing six edges of three different slopes, corresponds to a Farey triangle t_i. Triangles t_i and t_{i+1} share an edge e_i, whose endpoints are the shared slopes of S_i and S_{i+1}. If $\Omega_i = R$, the path from e_{i-1} to e_i takes a right turn across t_i; if $\Omega_i = L$, the path takes a left turn. This rule also defines an *initial edge* e_0, because $\Omega_1 = R$, so a right turn should take e_0 to e_1. Similarly, the action of Ω_c defines a *terminal edge* e_c.

For each e_i, $1 \leq i \leq c-1$, the 4–punctured spheres S_i and S_{i+1} are joined together along four edges, two for each endpoint of e_i. In between them lies a layer $\Delta_i = \Delta(e_i)$ of two tetrahedra, whose bottom surface S_i has the triangulation of t_i and whose top surface S_{i+1} has the triangulation of t_{i+1}. (See Figure 16 for an example.) Stacking these tetrahedron layers together produces a layered triangulation of the product region between S_1 and S_c.

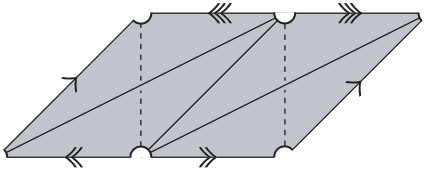

Figure 16: The tetrahedron layer $\Delta_1 = \Delta(e_1)$, made of two tetrahedra contained between 4–punctured spheres S_1 and S_2 (sides with identical arrows are identified)

If we wanted to construct a bundle of 4–punctured spheres over the circle, we would glue the top of this product region to the bottom. To recover the complement of the link $K(\Omega)$, we follow a slightly different procedure. On the 4–punctured sphere S_1,

corresponding to the first crossing inside the outer pillowcase, let the *peripheral edges* be the edges whose slope is the vertex of t_1 opposite the initial edge e_0.

We will fold S_1 along the two peripheral edges, identifying its ideal triangles in pairs. Figure 17 shows that this creates exactly the desired effect of connecting the strands of K in pairs, with a twist. This full twist corresponds to the first two crossings in the link projection: the first crossing in the braid, as well as the "extra" crossing outside the outer pillowcase. The four nonperipheral edges on S_1 are identified to a single edge, isotopic to a short arc near the crossing. The two ideal triangles that remain after folding are clasped together around this edge, which we call the *core* of the clasp.

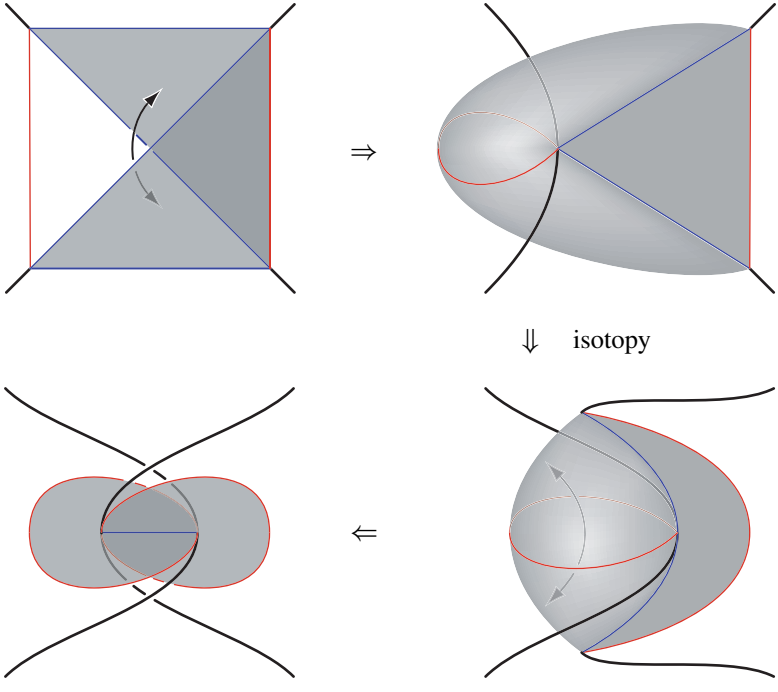

Figure 17: Folding the pleated surface S_1 produces the first two crossings in the link.

Let α be the mirror image of the peripheral slope across e_0 in the Farey graph. Topologically, folding S_1 as above amounts to attaching a thickened disk of boundary slope α to the outer pillowcase [23, Lemma II.2.5].

In a similar fashion, we define the peripheral edges on S_c to be the edges whose slope is the vertex of t_c opposite e_c. We fold S_c along these two peripheral edges, identifying

its faces to a clasp of two ideal triangles. Topologically, attaching 2–handles to S_1 and S_c results in a space homeomorphic to the link complement. Combinatorially, folding S_1 and S_c defines a gluing pattern for all the faces of the tetrahedra, giving us an ideal triangulation of $\mathbb{S}^3 \smallsetminus K$. See [23, Section II.2] for more details of this triangulation.

A.3 Combinatorics at the cusp

To describe the combinatorics of the boundary component(s) of $\mathbb{S}^3 \smallsetminus K$, we will first focus on the product region between the pleated surfaces S_1 and S_c. In the layered triangulation of this product region, each layer Δ_i consists of two tetrahedra, D_i and D_i', as in Figure 16. It is clear from the figure that each tetrahedron has exactly one vertex at each puncture of S_i, ie at each strand of the 4–string braid between S_1 and S_c. Since the combinatorics of the four strands are identical, let us focus on a single puncture of the 4–punctured sphere.

The tetrahedron layer Δ_i intersects the neighborhood of a puncture in two *boundary triangles*, one from a truncated vertex of D_i and one from D_i'. These boundary triangles meet at two vertices that come from shared edges of D_i and D_i'. (This completes a loop, corresponding to the meridian of a component of K.) The apices of the two triangles point in different directions, as in Figure 3. As with punctured torus bundles, these layers of boundary triangles are stacked together, forming fans that correspond to syllables of the word Ω.

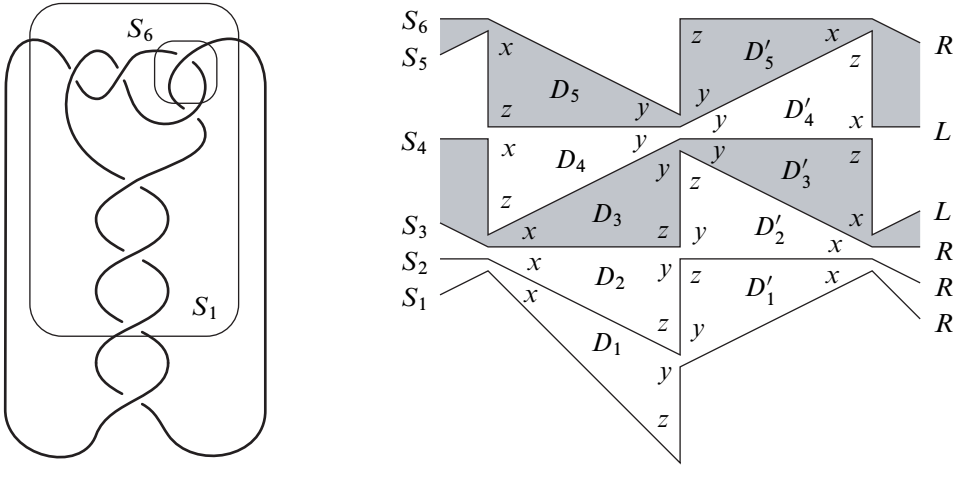

Figure 18: Left: the link $K(\Omega)$ corresponding to $\Omega = R^3 L^2 R$
Right: a cusp view of the product region between S_1 and S_c

The resulting cusp triangulation which corresponds to the product region of the link $K(R^3L^2R)$ is shown in Figure 18. As in Figure 4, the triangles are shown opened up, and the hinge layers are shaded. Observe that this picture is combinatorially equivalent to the corresponding picture for punctured torus bundles, quotiented by the hyperelliptic involution.

We have labeled the dihedral angles of the tetrahedra of Δ_i by numbers ("angles") x_i, y_i, z_i, following the same conventions as in Figure 4. Note that our choices of dihedral angles force the tetrahedra D_i and D_i' to be isometric; this does not impede the goal of finding a geometric triangulation. In the sequel, we will not distinguish between D_i and D_i'.

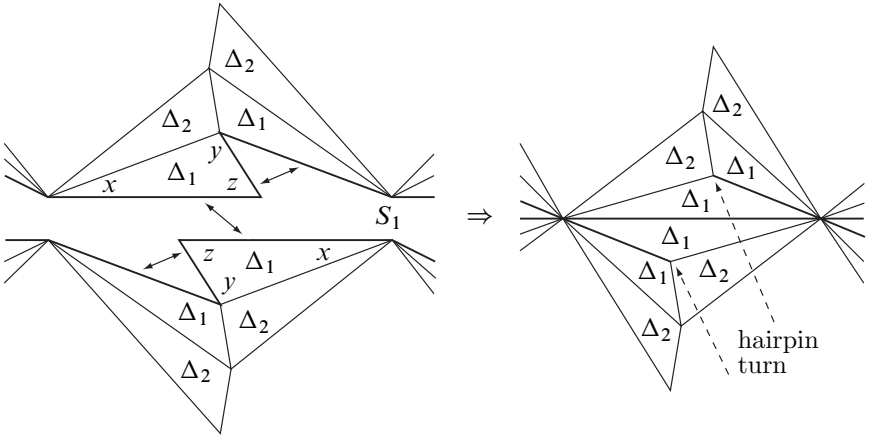

Figure 19: A cusp view of the folding that occurs at a clasp

When the pleated surface S_1 is folded to form a clasp, the zigzag line in which it intersects the cusp also becomes folded, creating a "hairpin turn." Because this folding procedure joins the punctures of S_1 in pairs, as in Figure 17, the boundary triangles on those punctures are also joined together. The resulting cusp triangulation in the neighborhood of S_1 can be seen in Figure 19. At the other end of the product region, the clasp of S_c appears on the cusp in the same way.

Once we have folded the clasp surfaces as prescribed, the truncated vertices of the tetrahedra combine to form either a single torus that traverses the product region four times (in case K is a knot), or two tori, each of which traverses the product region twice (in case K is a two-component link). In either case, the local combinatorics are the same, and the affine equations that the dihedral angles of the tetrahedra must satisfy are derived in the same way.

To find the hyperbolic structure on $\mathbb{S}^3 \smallsetminus K$, we will study the space P of *angle structures* for the triangulation, ie the space of positive dihedral angles that line up correctly around each edge. We need to complete three steps:

(1) Parameterize P and check that it is nonempty, as in Section 5.

(2) Show that a critical point of the volume functional on P gives a complete hyperbolic metric, as in Section 6.

(3) Prove that at any point on the boundary of $\bar{P}$, the volume can be increased by unflattening the flat tetrahedra, as in Section 7–Section 9.

This will imply that the volume functional is maximized in the interior of P, guaranteeing a critical point and thus a hyperbolic metric. For each of the three steps, the argument is essentially the same as Guéritaud's.

A.4 Angle structures and volume

Following Section 5 of the main article, we will parameterize the dihedral angles of the tetrahedra by *pleating angles* on the pleated 4–punctured spheres. Each sphere S_i described above has a natural transverse orientation that points (equivalently) toward the inside of the link projection, toward increasing indices, and upward in Figure 18. Just as in Section 5, for any edge $e \subset S_i$, we can define the *pleating angle* α to be the (signed) external angle at e, with signs chosen so that α is positive whenever the angle above e is less than π.

On the pleated sphere S_{i+1} living between Δ_i and Δ_{i+1}, this definition will give pleating angles

$$-2w_i, \quad 2w_{i+1} \quad \text{and} \quad 2w_i - 2w_{i+1},$$

exactly as in (2). The clasp surface S_1, which borders Δ_1 on one side and is folded on the other side, will have pleating angles $-\pi$, $2w_1$, and $\pi - 2w_1$, where the pleating angle of $-\pi$ corresponds to the hairpin turn in Figure 19. Thus, if we define $w_0 = \pi/2$ (even though there is no tetrahedron layer Δ_0), the pleating angles on S_1 will be given by the same expressions as above. Similarly, setting $w_c = \pi/2$ allows us to label the pleating angles on S_c by the same expressions as in (2).

Lemma A.2 *For $i = 0, \dots, c$, choose a parameter w_i, such that $w_0 = w_c = \pi/2$ and $w_1, \dots, w_{c-1}$ satisfy the range, concavity, and hinge conditions (3). For each such choice of parameters, set the dihedral angles of the tetrahedra as in Table 1. Then*

(1) *for each Δ_i, the angles x_i, y_i, z_i are positive and add up to π,*

(2) *the dihedral angles around each edge add up to 2π, and*

(3) *for each S_i, the pleating angles add up to 0.*

Proof The range, concavity, and hinge conditions imply that all the tetrahedron angles x_i, y_i, z_i are positive, and the claim that their sum is π is immediate from Table 1. For each pleated surface S_i, the pleating angles sum to 0 by construction. Therefore, it remains to check the angle sum around each edge e of $\mathbb{S}^3 \smallsetminus K$.

If e is not the core of S_1 or S_c, the combinatorial picture of Figure 18 is the same as the one for torus bundles. Thus, as in Section 5, each layer Δ_i contributes precisely the difference between the pleating angles of the neighboring surfaces, and the sum around e simplifies to 2π. If e is the core of a clasp, say the core of S_1, the left panel of Figure 19 shows that four sectors contribute dihedral angles at e: two sectors that have angle z_1, plus two fans of angles above pleated surface S_1, each having dihedral angle $2w_1$. Thus, because $z_1 + 2w_1 = \pi$, the total angle sum at e is 2π. □

By Lemma A.2, our triangulation will have an angle structure whenever we set $w_0 = w_c = \pi/2$ and interpolate between these parameters in a way that satisfies the range, concavity, and hinge conditions. One can always do this graphically, by first fixing w_i for the hinge indices and then connecting the hinges by pieces of parabolas, as in Figure 6 (this is where we use the hypothesis that Ω contains at least one hinge).

Lemma A.3 *Let P be the open affine polyhedron of angle structures for the triangulation of $\mathbb{S}^3 \smallsetminus K$, parameterized by sequences $(\frac{\pi}{2}, w_1, \dots, w_{c-1}, \frac{\pi}{2})$, as in Lemma A.2. Then a point of P is a critical point of the volume functional $\mathcal{V}$ if and only if the corresponding tetrahedron shapes give a complete hyperbolic structure on $\mathbb{S}^3 \smallsetminus K$.*

Just like Lemma 6.2, this is an instance of a much more general theorem of Rivin, Chan, and Hodgson [9; 22]. It is also possible to prove Lemma A.3 directly, using the same line of argument as in Lemma 6.2, although in the setting of two-bridge links this would require considering a number of special cases.

A.5 Flat tetrahedra never maximize volume

The proof that the maximum of $\mathcal{V}$ occurs in the interior of P closely tracks Section 7–Section 9 of Guéritaud's paper. We begin by ruling out many types of degeneracies on $\partial \bar{P}$.

Lemma A.4 *Let $(w_1, \dots, w_{c-1})$ be the point of $\bar{P}$ at which the volume functional $\mathcal{V}$ attains its maximum. Then (w_i) has the following properties:*

(1) *For each i, if one of x_i, y_i, z_i is 0, then two are 0, ie Δ_i is* flat.

(2) *If Δ_i is flat, then $w_i = 0$.*

(3) *If Δ_i is flat, then i is a hinge index, not equal to 1 or $c-1$.*

(4) *If Δ_i is flat, then i is adjacent to at least two consecutive identical letters.*

(5) *If both hinge layers at the ends of a syllable R^k or L^k are flat, then $k \geq 3$.*

Proof All the discussion and results of Section 7 apply equally well in our context. Thus we have conclusion (1) as a restatement of Proposition 7.1. The domino effect of Proposition 7.2 also applies; in fact, it is clear from the proof of the Proposition that the domino effect works both forward and backward. Thus it does not matter that our word Ω is not cyclic.

Almost all the claims of (2)–(5) are proved in Section 7, either in Proposition 7.3 or in the discussion that follows. The one exception is the claim that Δ_1 and Δ_{c-1} cannot flatten. This follows because, in the case of two-bridge links, $w_0 = w_c = \pi/2$. Thus setting w_1 or w_{c-1} to 0 or $\pi/2$ will trigger the domino effect and force all the tetrahedra to flatten, giving a volume of 0. □

It remains to prove that at any point $(w_i) \in \partial\overline{P}$ satisfying the properties of Lemma A.4, the volume will increase as we move into the interior of P. Following Guéritaud, we do this using the geometrical statement of Lemma 8.2. The proof of this lemma transfers perfectly to our context when the fan under consideration corresponds to a subword in the interior of Ω. As it turns out, the same statement is even easier to prove when the degenerate layer is near the beginning or end of Ω.

Lemma A.5 *Recall the word $\Omega = R^{a_1}L^{a_2}\cdots$, and suppose that the hinge layer Δ_{a_1} has flattened, with $w_{a_1} = 0$. Then the fan corresponding to $R^{a_1}L$ admits a complete Euclidean structure with boundary along S_{a_1}. Let Q, P, T be the lengths of the segments of the broken line in which S_{a_1} intersects the cusp, as in Figure 20. Then $Q < P + T$.*

Of course, the analogous statement holds near the end of Ω.

Proof Note that, by Lemma A.4, we have $a_1 \geq 2$. For all $1 \leq i \leq a_1 - 2$, the parameter w_i can vary in a small interval, and no generality is lost in assuming that $\partial\mathcal{V}/\partial w_i = 0$. (Otherwise, volume is easy to increase.) Then, as in the proof of Lemma 8.2, the criticality of volume with respect to these parameters implies that the fan of $R^{a_1}L$ has a complete Euclidean structure. If $i > 1$, the computation is the same as in Sublemma 6.4. If $i = 1$, the angle z_0 of Figure 7 is replaced by the hairpin turn, and the factor $\frac{\sin y_0}{\sin x_0}$ disappears from the computation of $\exp(-\partial\mathcal{V}/\partial w_1)$. Thus we once again have

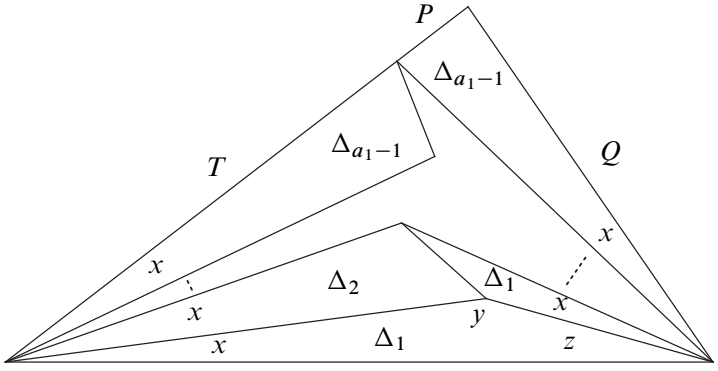

Figure 20: In a fan at the beginning of Ω, $Q < P + T$.

$1 = \exp(-\partial\mathcal{V}/\partial w_1) = |\psi(\alpha)|$, where ψ is the reduced holonomy and α is a loop around the vertex at the hairpin turn.

In our situation, the fan of $R^{a_1}L$ is a (tessellated) Euclidean triangle, as in Figure 20, in which Q and $P+T$ are two of the sidelengths. In the triangular fan, the angle opposite Q is $x_1 + \ldots + x_{a_1-1}$, while the angle opposite $P+T$ is $z_1 + x_1 + \ldots + x_{a_1-1}$. Thus, because its side is opposite the smaller angle, $Q < P + T$. □

Armed with Lemma 8.2 and its analogue in Lemma A.5, we can complete the proof of Theorem A.1 by following the argument of Section 9. For each hinge index j with $w_j = 0$, we pick a vector along which to deform the neighboring parameters, in a way that will maximize the derivative of volume. Deforming in this optimal direction with speed ε, we can compute $\partial\mathcal{V}/\partial\varepsilon$ in terms of the geometry of the fan(s) that adjoin Δ_j.

In most situations, the exponentiated derivative appears as a product of the exact same sine ratios as in Section 9. The only exception occurs when $j = 2$ or $j = c-2$, because there are no tetrahedra corresponding to w_0 or w_c. If (without loss of generality) $j = 2$, the angle z_0 is replaced by the hairpin turn, while the factor $\frac{\sin y_0}{\sin x_0}$ disappears from the computation of P/T, just as in the proof of Lemma A.5. Thus $\partial\mathcal{V}/\partial\varepsilon$ has the same expression in terms of Q, Q', P, P', T, T' as in Section 9.

In every case, the geometric statement $Q < P + T$, applied to two fans if necessary, implies that $\partial\mathcal{V}/\partial\varepsilon > 0$. Therefore $\mathcal{V}$ is maximized at a critical point where all tetrahedron angles are positive, completing the proof of Theorem A.1.

Appendix B Applications

Our construction of geometric triangulations using volume maximization methods has several corollaries that relate hyperbolic geometry (of bundles and links) to combinatorics (of the Farey complex and link diagrams).

B.1 Volume estimates for bundles

Theorem B.1 *Let V_φ be a once-punctured torus bundle defined by the cyclic word $\Omega = R^{a_1}L^{b_1}\cdots R^{a_n}L^{b_n}$. Then*

$$2n\,v_3 \;\le\; \mathrm{Vol}(V_\varphi) \;<\; 2n\,v_8,$$

where $v_3 \approx 1.0149$ is the volume of a regular ideal tetrahedron and $v_8 \approx 3.6638$ is the volume of a regular ideal octahedron. Both of these bounds are sharp.

This is a sharp, quantitative version of Brock's result in [8], in the special case of punctured torus bundles. The upper bound is not new; it is a special case of [2, Corollary 2.4].

Proof To prove the lower bound on volume, we exhibit a particular angle structure. It follows from the proof of Theorem 1.1 that the volume of the complete hyperbolic structure on V_φ is the global maximum of $\mathcal{V}$ over the closed polytope $\overline{P}$. Thus, for any $w \in \overline{P}$, $\mathcal{V}(w) \le \mathrm{Vol}(V_\varphi)$.

We choose w in the simplest possible manner: by letting $w_i = \frac{\pi}{3}$ for all i. It is easy to check that this choice of parameters satisfies at least the weak form of all the inequalities of (3). In other words, all angles are nonnegative, and $w \in \overline{P}$. Any nonhinge tetrahedron Δ_i will have one vanishing angle and will therefore have volume 0. However, every hinge tetrahedron Δ_i will be a regular tetrahedron, with all angles $\frac{\pi}{3}$ and volume v_3. Thus $\mathcal{V}(w) = 2nv_3$.

When $\Omega = (RL)^n$, and thus all tetrahedra are hinges, this choice of angles will in fact give the complete structure on V_φ. These bundles, which are n–fold cyclic covers of the figure–8 knot complement, have volume exactly $2nv_3$. On the other hand, the bundles that contain some nonhinge tetrahedra have $\mathrm{Vol}(V_\varphi) > 2nv_3$, because $\mathcal{V}$ is maximized at a point where all tetrahedra have positive angles.

To prove the upper bound, we employ a Dehn surgery construction. For every Farey vertex s which corresponds to a fan RL^*R or LR^*L (with $* > 0$), drill a closed curve of slope s out of the fiber at the corresponding level. (These are exactly the closed curves whose length was estimated in Section 10.) The resulting *drilled bundle* turns

out to be an n–fold cyclic cover of the Borromean rings complement, with volume $2nv_8$.

We can recover V_φ by Dehn filling the extra cusps of the drilled bundle. Because volume goes down under Dehn filling, $\mathrm{Vol}(V_\varphi) < 2nv_8$. If we pick a word Ω with very long syllables, as in Section 10, the resulting bundle V_φ has volume arbitrarily close to the volume of this surgery parent. □

Corollary B.2 *Let V_φ be a 4–punctured sphere bundle defined by the cyclic word $\Omega = R^{a_1}L^{b_1}\cdots R^{a_n}L^{b_n}$. Then*

$$4n\,v_3 \;\le\; \mathrm{Vol}(V_\varphi) \;<\; 4n\,v_8.$$

B.2 Volume estimates for links

The volumes of link complements can also be estimated in terms of diagrams. We say that a link diagram D is *reduced* if no single crossing separates D. Its *twist number* $\mathrm{tw}(D)$ is the number of equivalence classes of crossings, where two crossings are considered equivalent if there is a loop in the projection plane intersecting D transversely precisely in the two crossings. When the diagram D depicts a two-bridge link constructed from a braid, as in Figure 13, $\mathrm{tw}(D)$ is precisely the number of syllables of the word Ω describing the braid.

Theorem B.3 *Let D be a reduced alternating diagram of a hyperbolic two-bridge link K. Then*

$$2v_3\,\mathrm{tw}(D) - 2.7066 \;<\; \mathrm{Vol}(\mathbb{S}^3\smallsetminus K) \;<\; 2v_8(\mathrm{tw}(D)-1).$$

The upper bound is sharp, and the lower bound is asymptotically sharp.

There are known diagrammatic volume bounds for the general class of alternating links. On the lower side, Agol, Storm, and W Thurston proved that the volume of an alternating link is at least $\frac{v_8}{2}(\mathrm{tw}(D)-2)$ [3], improving an earlier bound due to Lackenby [14]. On the upper side, Agol and D Thurston proved an asymptotically sharp bound of $10v_3(\mathrm{tw}(D)-1)$ [14, Appendix]. Numerically, Theorem B.3 improves the multiplicative constant in the lower bound from 1.8312 to 2.0299 and the multiplicative constant in the upper bound from 10.1494 to 7.3277 (in the special case of 2–bridge links).

Compared to its predecessors, Theorem B.3 is less general, but uses only very elementary methods. The proof in [3] relies in a fundamental way on Perelman's results about the monotonicity of volume under Ricci flow with surgery. By contrast, the lower bound in Theorem B.3 only relies on the explicit study of angled triangulations.

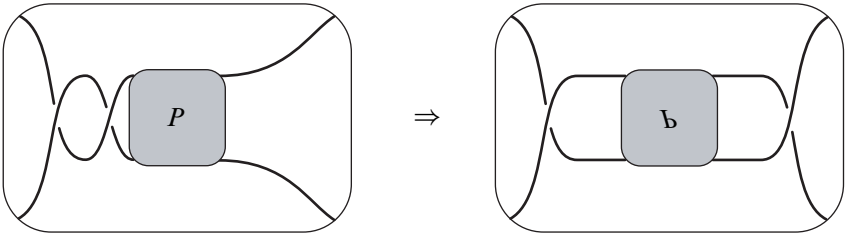

Figure 21: A flype in a diagram of a two-bridge link. The shaded rectangle P is a pillowcase of the braid.

Proof First, we claim that it suffices to consider a diagram D like the one in Figure 13, constructed from an alternating braid with one free strand. By the Menasco–Thistlethwaite flyping theorem [16], any pair of reduced alternating diagrams of K are related by a sequence of *flypes*, as in Figure 21. It is easy to check that the twist number of a diagram is invariant under flypes. Thus the number of syllables of the word Ω is the twist number of *any* reduced alternating diagram of K.

Lower bound Suppose that the link is defined by the word $\Omega = R^{a_1} L^{a_2} \cdots R^{a_n}$ (the parity of $n = \mathrm{tw}(D)$ and the letter of the first and last syllables are unimportant). As in the proof of Theorem B.1, we explicitly choose a point $w = (\frac{\pi}{2}, w_1, \ldots, w_{c-1}, \frac{\pi}{2})$ of $\overline{P}$. However, the concavity condition of (3) does not allow us to set $w_i = \frac{\pi}{3}$ when i is too close to 0 or c. Instead, we proceed as follows. We let $w_i = \frac{\pi}{3}$ for all $a_1 \le i \le c - a_n$. For the indices of the first and last fans, we interpolate linearly between $\frac{\pi}{2}$ and $\frac{\pi}{3}$. As before, it is easy to check that these values of the parameters make all tetrahedron angles nonnegative, and give us a point of $\overline{P}$.

When i is a hinge and $a_1 < i < c - a_n$, the two tetrahedra of Δ_i have all dihedral angles $\frac{\pi}{3}$, and volume v_3. For $n \ge 3$, there are exactly $n-3$ hinge indices of this type. When $i = a_1$ or $i = c - a_n$, we can compute from Table 1 that the three angles of Δ_i are

$$\frac{\pi}{3} + t_i, \quad \frac{\pi}{3} - t_i \quad \text{and} \quad \frac{\pi}{3}, \quad \text{where} \quad t_i = |w_{i+1} - w_{i-1}| \le \frac{\pi}{6}.$$

By Proposition 6.6, the volume defined by these angles is smallest at the extreme value of $t_i = \frac{\pi}{6}$, when the three angles are $\frac{\pi}{2}, \frac{\pi}{3}, \frac{\pi}{6}$. Still assuming $n \ge 3$, by Formula (4) the four tetrahedra in the two terminal hinge layers each have volume at least $0.84578\ldots$ Putting it all together gives

$$\mathcal{V}(w) \;>\; 2v_3\,(\mathrm{tw}(D) - 3) + 4 \times 0.84578 \;>\; 2v_3\,\mathrm{tw}(D) - 2.7066.$$

(As a special case, if $n = 2$, $\mathcal{V}(w) > 2 \times 0.84578$ also satisfies the theorem.)

To prove that this bound is asymptotically sharp, let $\Omega = (RL)^k$, for large k. Then $\mathrm{tw}(D) = 2k$, and the triangulation of $K(\Omega)$ consists of $2(\mathrm{tw}(D)-1)$ tetrahedra, all of them hinges. Since the volume of an ideal tetrahedron is bounded above by v_3, $\mathrm{Vol}(\mathbb{S}^3 \setminus K) \leq 2v_3(\mathrm{tw}(D)-1)$, a value whose ratio to the lower bound of the theorem approaches 1 as $\mathrm{tw}(D)$ gets large.

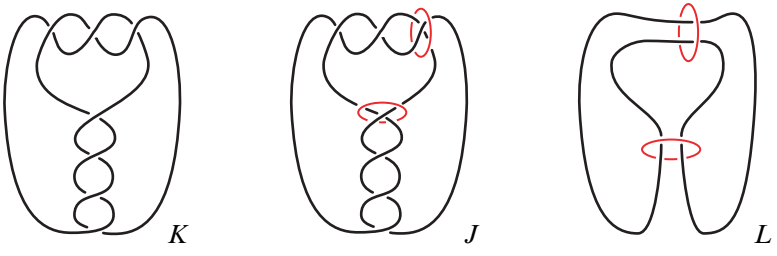

Figure 22: The construction of an augmented 2–bridge link L. When $\mathrm{tw}(D) = 2$, L is the Borromean rings.

Upper bound The proof of the upper bound uses the same surgery argument that Lackenby, Agol, and Thurston used for general alternating links [14], and the improved estimate comes from the special structure of 2–bridge links.

Let D be a diagram as in Figure 13. Recall that each syllable of Ω corresponds to a *twist region* where two strands of the braid wrap around each other. For every twist region, we add an extra link component (called a *crossing circle*) encircling the two strands of K, obtaining a hyperbolic link J [14]. (See Figure 22.) Every crossing circle of J bounds a *crossing disk* that is punctured by the two strands of K. Because twice-punctured disks are totally geodesic [1], we can untwist all the crossings in the twist region and obtain a new link L, called an *augmented link*, whose volume is equal to that of J.

When K is a two-bridge link, L has the following alternate description. Start with $(\mathrm{tw}(D)-1)$ copies of the Borromean rings, cut each one along a crossing disk, and glue the copies together in a linear fashion. Volume is additive under this operation [1]. Thus $\mathrm{Vol}(\mathbb{S}^3 \setminus L) = 2v_8(\mathrm{tw}(D)-1)$, since the Borromean rings have volume $2v_8$. Since K is obtained by Dehn filling the crossing circles of J, we have

$$\mathrm{Vol}(\mathbb{S}^3 \setminus K) \;<\; \mathrm{Vol}(\mathbb{S}^3 \setminus J) \;=\; \mathrm{Vol}(\mathbb{S}^3 \setminus L) \;=\; 2v_8(\mathrm{tw}(D)-1).$$

By choosing a link with many crossings in each twist region, one can get $\mathrm{Vol}(\mathbb{S}^3 \setminus K)$ arbitrarily close to this upper bound. □

B.3 Hyperbolic geodesics seen in the projection plane

For any link diagram D, a *crossing arc* is a segment perpendicular to the projection plane that connects the upper strand of a crossing to the lower strand of the same crossing. Morwen Thistlethwaite has conjectured that in any reduced alternating diagram of a hyperbolic link K, every crossing arc is isotopic to a hyperbolic geodesic. As a consequence of Theorem A.1, we can prove this in the case of two-bridge links.

Theorem B.4 *Let D be a reduced alternating diagram of a hyperbolic two-bridge link K. Then every crossing arc of D is isotopic to an edge in the Sakuma–Weeks triangulation of $\mathbb{S}^3 \smallsetminus K$, and thus to a geodesic.*

In fact, still more is true: each edge of the triangulation is dual to a face of the Ford–Voronoi domain of $\mathbb{S}^3 \smallsetminus K$ [5].

Proof We begin by observing that the statement is true for a diagram D_0 as in Figure 13, constructed from an alternating braid with one free strand. Every crossing of D_0 corresponds to a 4–punctured sphere pleated along edges of our triangulation. As Figure 15 illustrates, the crossing arc of any crossing is isotopic to one of the edges.

As it turns out, the diagram D_0 is not overly special. Thistlethwaite has proved that every reduced alternating diagram D of a two-bridge link is standard: that is, D can also be constructed from an alternating 4–string braid, although not necessarily with a free strand [24, Theorem 4.1]. Furthermore, by the Menasco–Thistlethwaite flyping theorem [16], we can get from D_0 to D by performing a sequence of *flypes* along the pillowcases of the braid. (See Figure 21.) During each flype, the diagram loses a crossing whose crossing arc is isotopic to an edge e of the triangulation, and gains another crossing, whose arc is isotopic to an edge e' of the same slope as e. Thus the crossing arcs of every diagram are isotopic to geodesics. □

References

[1] **C C Adams**, *Thrice-punctured spheres in hyperbolic 3–manifolds*, Trans. Amer. Math. Soc. 287 (1985) 645–656 MR768730

[2] **I Agol**, *Small 3–manifolds of large genus*, Geom. Dedicata 102 (2003) 53–64 MR2026837

[3] **I Agol**, **P Storm**, **W Thurston**, *Lower bounds on volumes of hyperbolic Haken 3–manifolds* arXiv:math.DG/0506338

[4] **H Akiyoshi**, *On the Ford domains of once-punctured torus groups*, Sūrikaisekikenkyūsho Kōkyūroku (1999) 109–121 MR1744475

[5] **H Akiyoshi**, **M Sakuma**, **M Wada**, **Y Yamashita**, *Ford domains of punctured torus groups and two–bridge knot groups*, from: "Knot Theory: dedicated to 70th birthday of Prof. Kunio Murasugi", (M Sakuma, editor) (2000)

[6] **H Akiyoshi**, **M Sakuma**, **M Wada**, **Y Yamashita**, *Jørgensen's picture of punctured torus groups and its refinement*, from: "Kleinian groups and hyperbolic 3–manifolds (Warwick, 2001)", London Math. Soc. Lecture Note Ser. 299, Cambridge Univ. Press, Cambridge (2003) 247–273 MR2044553

[7] **P Alestalo**, **H Helling**, *On torus fibrations over the circle*, Sonderforschungsbereich SFB-343 (1997)

[8] **J F Brock**, *Weil–Petersson translation distance and volumes of mapping tori*, Comm. Anal. Geom. 11 (2003) 987–999 MR2032506

[9] **K Chan**, *Constructing hyperbolic 3–manifolds*, Undergraduate thesis, University of Melbourne (2002) with C Hodgson

[10] **F Guéritaud**, *Triangulated cores of punctured–torus groups* arXiv:math.GT/0605481

[11] **H Helling**, *The trace fields of a series of hyperbolic manifolds*, Sonderforschungsbereich SFB-343 (1999)

[12] **T Koch**, *Fordsche Fundamentalbereiche hyperbolischer einfach-punktierter Torus-Bündel*, Sonderforschungsbereich SFB-343 (1999)

[13] **M Lackenby**, *The canonical decomposition of once-punctured torus bundles*, Comment. Math. Helv. 78 (2003) 363–384 MR1988201

[14] **M Lackenby**, *The volume of hyperbolic alternating link complements,* With an appendix by Ian Agol and Dylan Thurston, Proc. London Math. Soc. (3) 88 (2004) 204–224 MR2018964

[15] **W Menasco**, *Closed incompressible surfaces in alternating knot and link complements*, Topology 23 (1984) 37–44 MR721450

[16] **W Menasco**, **M Thistlethwaite**, *The classification of alternating links*, Ann. of Math. (2) 138 (1993) 113–171 MR1230928

[17] **J Milnor**, *Hyperbolic geometry: the first 150 years*, Bull. Amer. Math. Soc. (N.S.) 6 (1982) 9–24 MR634431

[18] **Y N Minsky**, *The classification of punctured-torus groups*, Ann. of Math. (2) 149 (1999) 559–626 MR1689341

[19] **K Murasugi**, *Knot theory and its applications*, Birkhäuser, Boston (1996) MR1391727

[20] **W D Neumann**, **D Zagier**, *Volumes of hyperbolic three-manifolds*, Topology 24 (1985) 307–332 MR815482

[21] **J-P Otal**, *Le théorème d'hyperbolisation pour les variétés fibrées de dimension 3*, Astérisque (1996) x+159 MR1402300

[22] **I Rivin**, *Euclidean structures on simplicial surfaces and hyperbolic volume*, Ann. of Math. (2) 139 (1994) 553–580 MR1283870

[23] **M Sakuma**, **J Weeks**, *Examples of canonical decompositions of hyperbolic link complements*, Japan. J. Math. (N.S.) 21 (1995) 393–439 MR1364387

[24] **M B Thistlethwaite**, *On the algebraic part of an alternating link*, Pacific J. Math. 151 (1991) 317–333 MR1132393

[25] **Y Colin de Verdière**, *Un principe variationnel pour les empilements de cercles*, Invent. Math. 104 (1991) 655–669 MR1106755

DMA, École normale supérieure, CNRS
45 rue d'Ulm, 75005 Paris, France

D Futer: *Mathematics Department, Michigan State University*
East Lansing, MI 48824, USA

gueritau@dma.ens.fr, dfuter@math.msu.edu

Proposed: Walter Neumann
Seconded: Jean-Pierre Otal, Joan Birman
Received: 10 November 2005
Revised: 29 July 2006